NAVAL PROVING GROUND

DAHLGREN, VIRGINIA

REPORT NO. 9-46

ANALYTICAL SUMMARY PART IV
THE THEORY OF ARMOR PENETRATION

1 May 1946

NAVAL PROVING GROUND

DAHLGREN, VIRGINIA

Captain David I. Hedrick, USN
Commanding Officer

Captain K. M. McLaren, USN
Ordnance Officer

NPG Report No. 9-46

ANALYTICAL SUMMARY PART IV
THE THEORY OF ARMOR PENETRATION

A. V. HERSHEY
Lieutenant, USNR

1 May 1946

NPG Report No. 9-46

ANALYTICAL SUMMARY PART IV
The Theory of Armor Penetration

1. For some years the Naval Proving Ground has been assiduously engaged in the study of the penetration of armor by projectiles. Pursuance of this work to conclusive results must be predicated upon well substantiated theories defining the performances of the materials involved under the various possible conditions.

2. Particularly necessary in the more immediately practical field of armor study and evaluation is the need for dependable plate penetration charts or tables. In 1943 Lieut. A. V. Hershey, USNR was assigned the task of preparing such charts. In prosecution of the assigned task he conducted an exhaustive study, employed for the first time new methods of attack and developed new theories concerning the phenomena incident to the penetration of plates by projectiles.

3. During the latter years of World War II, Lieut Hershey prepared a series of nine reports which are being published by the Naval Proving Ground under titles as follows:

(1) ANALYTICAL SUMMARY. PART I. THE PHYSICAL PROPERTIES OF STS UNDER TRIAXIAL STRESS.

Object: To summarize the available data on the physical properties of Class B Armor and STS under triaxial stress.

(2) ANALYTICAL SUMMARY. PART II. ELASTIC AND PLASTIC UNDULATIONS IN ARMOR PLATE.

Object: To analyse the propagation of undulations in armor plate; to summarize previous analytical work and to add new analytical work where required in order to complete the theory for ballistic applications.

(3) ANALYTICAL SUMMARY. PART III. PLASTIC FLOW IN ARMOR PLATE.

Object: To analyse the plastic flow in armor plate adjacent to the point of impact by a projectile.

(4) ANALYTICAL SUMMARY. PART IV. THE THEORY OF ARMOR PENETRATION.

Object: To summarize the theory of armor penetration in its present state of development, and to develop theoretical functions which can be used as a guide in the interpretation of ballistic data.

(5) BALLISTIC SUMMARY. PART I. THE DEPENDENCE OF LIMIT VELOCITY ON PLATE THICKNESS AND OBLIQUITY AT LOW OBLIQUITY.

Object: To compare the results of ballistic test with the prediction of existing formulae, and with the results of theoretical analysis; to find the mathematical functions which best represent the fundamental relationship between limit velocity, plate thickness, and obliquity at low obliquity.

(6) BALLISTIC SUMMARY. PART II. THE SCALE EFFECT AND THE OGIVE EFFECT.

Object: To determine the effect of scale on ballistic performance, and to correlate the projectile nose shape with the results of ballistic test.

(7) BALLISTIC SUMMARY. PART III. THE WINDSHIELD EFFECT, AND THE OBLIQUITY EFFECT FOR COMMON PROJECTILES.

Object: To analyse the action of a windshield during impact, and to develop mathematical functions which best represent the ballistic performance of common projectiles.

(8) BALLISTIC SUMMARY. PART IV. THE CAP EFFECT, AND THE OBLIQUITY EFFECT FOR AP PROJECTILES.

Object: To determine the action of a cap during impact, and to develop mathematical functions which best represent the ballistic performance of AP projectiles.

(9) BALLISTIC SUMMARY. PART V. THE CONSTRUCTION OF PLATE PENETRATION CHARTS OR TABLES.

Object: To summarize the results of analysis in the form of standard charts or tables.

4. The opinions and statements contained in these reports are the expressions of the author, and do not necessarily represent the official views of the Naval Proving Ground.

David I. Hedrick.

DAVID I. HEDRICK
Captain, USN
Commanding Officer

P R E F A C E

AUTHORIZATION

The material in this report is supplementary to the construction of plate penetration charts. It was authorized by Buord letter NP9/A9 (Re3) dated 9 January 1943.

OBJECT

To summarize the theory of armor penetration in its present state of development, and to develop theoretical functions which can be used as a guide in the interpretation of ballistic data.

SUMMARY

The major phenomena of armor penetration are described. Formulae for elastic undulations in a thin membrane and a thick plate are combined into a simple formula whose algebraic form is consistent with direct experiments on elastic undulations in plates of intermediate thickness. Force-penetration curves for 3" AP M79 projectiles are derived from the depth of penetration of projectiles into homogeneous plate at impact velocities less than the limit velocity. The force-penetration curves are used in the qualitative analysis of plate boundary effects, and are used in the determination of the distribution of impact energy between the elastic undulation in the plate and the plastic deformation near the impact.

A theory is developed to represent the limiting case of a thin plate. The thin plate theory is based on the following simplifications:

(a) The energy required to crack the plate is assumed to be proportional to the imbedded volume of the projectile with the tip of the nose just at the back of the plate. The average pressure on the projectile before fracture of the plate is assumed to be equal to the average pressure in the equilibrium expansion of a hole of uniform diameter. The thickness of the plate near the point of impact, just at fracture, is assumed to be equal to the thickness of the plate near a hole of uniform diameter.

(b) The energy required to push back the petals after fracture is assumed to be proportional to the plate thickness.

(c) The energy delivered to the transverse undulation by the projectile is assumed to be the same as the energy in an elastic undulation with the force concentrated at a point.

A theory is developed to represent the limiting case of a thick plate. The thick plate theory is based on the following simplifications:

(a) The medium is assumed to exert no shear stress in a zone next to the impact hole where faults can occur.

(b) The plastic energy per unit volume of armor in the path of the projectile is assumed to be constant through the thickness of the plate, in the zone of irrotational flow, but is assumed to be the same as the energy in the equilibrium expansion of a hole in a thin plate with free surfaces, in the zone of equilibrium flow. The total plastic energy is assumed to be half the sum of the limiting energies for irrotational flow and equilibrium flow.

(c) The energy delivered to the transverse undulation is assumed to be the same as the energy in an elastic undulation with the force concentrated at a point.

TABLE OF CONTENTS

LIST OF TABLES

LIST OF FIGURES

I INTRODUCTION

A theoretical analysis of armor penetration has a twofold purpose. It leads to an understanding of the mechanism of armor penetration, an understanding which may stimulate the discovery of improved methods of manufacture or design. It provides a rational basis for the construction of penetration charts, especially for ballistic conditions which have not been fully investigated by an unlimited number of tests. A penetration chart which is based on a combination of theory and test is more likely to be correct in the end than one based on a blind empirical correlation of data which are badly scattered and cover only a limited range of test condition.

The theoretical analysis of armor penetration consists in the recognition of the various forms of energy which are taken up by the armor during impact, and the evaluation of these forms of energy in terms of known relationships between stress, strain and rate of strain.

An exact theory of armor penetration is at present beyond the scope of the solitary analyst with only the conventional aids to calculation, but the major phenomena in armor penetration may nevertheless be outlined by a qualitative theory. An exact theory is possible for certain idealized systems which resemble armor penetration such as those in Table I, and may be used to calibrate the major phenomena with the aid of fundamental assumptions which are dictated by the qualitative theory. The semiquantitative theory which is thus obtained does not agree exactly with the ballistic data, but does serve as a guide to the best choice of mathematical functions to represent the test results.

Major contributions to the present theory of armor penetration have been made by vonKarman[1] at the California Institute of Technology, who first investigated the propagation of plastic waves in bars, and by Zener[7] at Watertown Arsenal, who first identified the conditions for failure by shear with the maximum in the adiabatic stress-strain curve for shear, and also published[8] the first analysis of friction between plate and projectile. Details of the propagation of flexural undulations in plates have been published at the California Institute of Technology[2], while details of the propagation of extensional undulations in membranes have been contributed by the Naval Proving Ground[15]. The radial expansion of a cylindrical hole in a thin plate was first published by Bethe[6] for a medium without work-hardening and has since been generalized at the Naval Proving Ground to include any arbitrary rate of work-hardening. The irrotational flow of armor near a projectile in a plate of caliber thickness and in an infinite medium has been analysed at the Naval Proving Ground[16].

The semiquantitative theory in its present state is applied in the present report to the penetration of 3" AP M79 projectiles at low obliquity into STS with a tensile strength of 115000 (lb)/(in)^2.

A knowledge of the relationship between the force on the projectile and its penetration into a plate is required in the analysis of armor penetration. Direct measurements have been made at the Naval Research Laboratory[8] on cal. .27 AP darts with a 2.5 cal. ogival radius, but no measurements are available for projectiles similar to the 3" AP M79 projectile whose ogival radius is 1.67 cal. Force-penetration curves for the 3" projectile have therefore been laboriously derived from the depth of penetration of projectiles into homogeneous armor during incomplete penetrations.

II THE BALLISTIC PARAMETERS

The analysis of armor penetration may conveniently be summarized in terms of a number of ballistic parameters. The impact parameter F_S, the plate penetration coefficient $F(e/d,\theta)$ and the residual velocity function F_R, may all be defined in terms of the projectile mass m, the projectile diameter d, the plate thickness e, the obliquity θ, the striking velocity v_S, the limit velocity v_L, and the remaining velocity v_R by the equation

$$F_S = \frac{m^{\frac{1}{2}} v_S \cos\theta}{e^{\frac{1}{2}} d}$$

$$F(e/d,\theta) = \frac{m^{\frac{1}{2}} v_L \cos\theta}{e^{\frac{1}{2}} d}$$

$$F_R = \frac{m^{\frac{1}{2}} v_R \cos\theta}{e^{\frac{1}{2}} d}$$

These parameters are convenient to use in the representation of ballistic performance since they are directly proportional to velocity, and do not vary rapidly with plate thickness or obliquity.

Of more fundamental significance are the impact energy parameter U_S, the limit energy function $U(e/d,\theta)$ and the residual energy function U_R which are defined in terms of F_S, $F(e/d,\theta)$ and F_R by the equations

$$U_S = \left(\frac{e}{d}\right)F_S^2$$

$$U(e/d,\theta) = \left(\frac{e}{d}\right)F^2\left(\frac{e}{d},\theta\right) = \frac{mv_L^2\cos^2\theta}{d^3}$$

$$U_R = \left(\frac{e}{d}\right)F_R^2$$

These parameters are proportional to the kinetic energy of the projectile at normal obliquity.

Another series of parameters which are useful in the interpretation of absorption data are the parameters F_S^2, $F^2(e/d,\theta)$, and F_R^2. The parameter $F^2(e/d,\theta)$ is proportional to the average pressure on the projectile during impact at normal obliquity.

Ballistic performance may be interpreted with equal validity in terms of any one of the three functions $F(e/d,\theta)$, $F^2(e/d,\theta)$, or $U(e/d,\theta)$. The projectile mass in the functions is expressed in (lb), the projectile diameter is given in (ft), the plate thickness in (ft) and the velocity of the projectile in (ft)/(sec).

The limit energy function[17] for the standard 3" AP M79 projectile at low obliquity is given by the equation

$$U(e/d,\theta) = \left(\frac{e}{d}\right)\Phi^2\theta\cos\theta$$

in which Φ is a function of e/d and θ is a function of θ. The functions Φ and θ are illustrated graphically by Figures (1) and (4), and the limit energy function is tabulated in Table III.

III GENERAL THEORY

The stress-strain relationships[14] for slow isothermal flow are all similar in the three limiting cases of shear, tension, and compression, and the stress-strain relationships for intermediate cases may be found from the limiting cases by interpolation. There appears to be no evidence that armor steel is anisotropic, although it is often inhomogeneous. The principal axes of stress are probably therefore collinear with the principal axes of strain rate. The components of stress for rapid plastic flow are greater than the components of strain for slow plastic flow by a factor which increases slowly with the strain rate. The shear stress in armor steel decreases with increase in temperature, and increases with increase in normal pressure. The stress-strain curve for shear, during adiabatic flow, passes through a maximum as the strain increases.

The work done on unit volume of the medium is not a single valued function of the final strain, but depends also on the path of deformation. Pure compression with simultaneous rotation of the principal axis of compression through 180°, produces nearly the same final strain as pure shear with stationary principal axes of strain, yet the plastic work is nearly twice as great.

Any disturbance in the interior of a solid medium is propagated by two waves which move with different velocities. The leading wave is a compressional or longitudinal wave, while the trailing wave is an equivoluminal or transverse wave. The velocity of propagation of the longitudinal wave is determined primarily by the bulk modulus of the medium and remains finite for any strain. The velocity of propagation of the transverse wave is derived from the stress-strain curve for shear, and decreases to zero as the strain in the medium approaches the strain for maximum stress.

A longitudinal wave in a solid medium is not isotropic. Transverse and longitudinal waves are therefore both reflected when a longitudinal wave reaches a free surface. The principal axes of stress at a free surface are always parallel to the surface, and the principal component of stress normal to the surface is zero. A line in the medium which was initially orthogonal to a free surface continues to be orthogonal during any distortion of the free surface.

A transverse undulation is created in a plate at the point of impact, and is propagated rapidly away over the surface of the plate.[15] If the undulation is elastic, it is maintained by a force, which increases with increase in both the velocity and displacement of the plate at the point of application of force.

If the plate is finite in extent, and is, in fact, so small that the elastic undulation reaches the edge of the plate during the application of force, then the energy in the plate of finite extent differs by a small amount from the energy in a plate of infinite extent, and the method of support at the border has a small effect on the energy. The elastic undulation in the limiting case of a thin plate is propagated at a finite rate only in the presence of a tension stress, which is built up by the undulation itself. If the plate is rigidly clamped at the border, the tension stress in the finite plate builds up more rapidly than it does in an infinite plate, the displacement normal to the initial plane is smaller, and the elastic energy is less. On the otherhand, if the plate is supported by a knife edge, or is suspended free, the tension stress at the border is zero, and the tension stress in the finite plate builds up more slowly than it does in an infinite plate, the displacement is larger, and the elastic energy is greater. The elastic undulation in the limiting case of a thick plate is propagated by a flexural rigidity, which is independent of the amplitude of undulation. The method of support should have no appreciable effect on the energy in a thick plate unless the plate is so small that the elastic undulation is reflected from the border and returns to the center of the plate during the application of force.

The momentum and energy transferred to the elastic undulation are greatest in a limit impact, which lasts longer than either an incomplete penetration or a complete penetration.

The pressure on the nose of the projectile in a limit impact is more than the plate material can stand without plastic flow. The plate material in the path of the projectile is forced outward toward the nearest free surface, and the plate is increased in thickness around the point of impact. The volume of plate material in the path of the projectile is directly proportional to the plate thickness and inversely proportional to the cosine of the angle of obliquity. The amount of plastic flow is determined by the volume of plate material in the path of the projectile, but the distribution of plastic flow is determined by the proximity of the free surfaces. The plastic flow is thus concentrated near the point of impact in a thin plate, but is spread out to a greater radius in a thick plate. The plastic flow is symmetric about an impact at normal obliquity, but is concentrated around the side nearest to the plate normal at other obliquities. The plastic energy in a limit impact at low obliquity is almost inversely proportional to the cosine of the obliquity but not quite, because the distribution of plastic flow changes with obliquity. The plastic energy in a limit impact at high obliquity on the other hand, increases more rapidly with obliquity because of projectile ricochet.

The velocity of propagation of a longitudinal wave in the armor is always many times greater than the velocity of the projectile. The velocity of propagation of a transverse wave is initially also greater than the velocity of the projectile, but decreases during impact as the plastic flow proceeds. Multiple reflections of the transverse waves between the faces of a thin plate maintain the medium near the point of impact in a state of equilibrium. Dynamics in a thin plate are only important at the outer radius of the elastic undulation. The transverse waves in a thick plate, however, are not quite able to maintain the medium in a state of equilibrium. The velocity of propagation of a transverse wave in a thick plate decreases toward the point of impact and is zero at a distance of one tenth caliber from the surface of the impact hole. The transverse waves originate at the free surfaces of the plate and move inward, but there is a zone next to the impact hole which is reached only by longitudinal waves. The medium in this zone is maintained in a state of steady irrotational flow.

Plastic flow in the armor is maintained at a finite rate by a steady stress system, which is a function of the state of strain, and increases slowly with increase in rate of strain, but is nearly independent of the acceleration of the medium. The armor is accelerated out of the way of the projectile by a dynamic stress system, which is superimposed on the steady stress. During the early stages of the penetration cycle the armor adjacent to the point of impact is undergoing a net acceleration and the total force applied by the plate to the projectile is greater than the force applied by the steady stress alone. During the later stages of the penetration cycle, the armor adjacent to the point of impact is undergoing a deceleration along with the projectile, and the total force applied to the projectile is less than the force applied by the steady stress alone. During an incomplete penetration there is an instant when the projectile has been brought to rest, after which the projectile begins to be rejected by an elastic reaction. At the instant when the projectile is at rest, the material in the plate adjacent to the point of impact is also at rest. The momentum temporarily transferred from the projectile to the armor by the dynamic stress has nearly all been returned to the projectile. The entire momentum of the projectile has been transmitted, by the steady stress, to the elastic undulation where it is radiated off. The kinetic energy temporarily transferred to the armor by the dynamic stress has also all been restored to the projectile, except for a small amount which is radiated off. A large amount of internal energy is retained by the armor adjacent to the point of impact in the form of heat, but no kinetic energy is retained. The armor at the surface of the projectile is heated to a high temperature and the shear stress at the surface is reduced until the friction between plate and projectile is nearly eliminated.[8,13]

There are two types of dynamic stress, a transient pressure which moves with the velocity of a longitudinal wave, and sets the medium into a state of flow, and a steady pressure which maintains the acceleration of the medium within the steady flow.

The first type of dynamic stress is generated partly at the rim of the coronet by the spreading of the rim, and partly over the nose of the projectile by the deceleration of the projectile. The distribution of transient pressure in the medium depends upon the shape of the ogive. A flat nosed cylindrical projectile generates a pressure pulse with a plane wave front behind which the pressure is initially very great. Diffraction at the perimeter of the wave front reduces the pressure behind the wave front as the wave advances. The pressure wave is reflected from the back of the plate as a tension wave which cancels the pressure. A high pressure pulse of limited extent is generated near the tip of a round nosed projectile, where the rim of the coronet moves with a velocity greater than the velocity of a longitudinal wave, but the rest of the transient pressure from a round nosed projectile varies gradually from point to point in the medium. All of the transient pressure from a pointed projectile varies gradually since the velocity of a longitudinal wave is many times greater than the velocity of the rim of the coronet.

The second type of dynamic stress is a steady or Bernoullian pressure[10,18], which is positive and greatest at the tip of the nose of the projectile, but is negative and least near the sides of the nose. Its total contribution to the force on the projectile in the absence of cavitation is zero. The Bernoullian pressure varies as the square of the velocity of the projectile. If, therefore, the velocity is increased, the negative pressure at the sides of the nose becomes great enough to cancel the steady plastic stress, and cavitation begins. At a velocity greater than the critical velocity for cavitation, the projectile blasts a hole in the plate with a larger diameter than the diameter of the projectile, and the energy required per unit length of hole is greater than it is in the absence of cavitation.

The strain at any particular point in the neighborhood of the impact hole is, at any particular stage of the penetration cycle, nearly independent of the velocity of the projectile, whereas the rate of strain at the point is nearly proportional to the velocity of the projectile. The steady stress at the point varies logarithmically with the rate of strain. The force on the projectile applied by the steady stress varies therefore also logarithmically with the velocity of the projectile.

The tension-extension relationship in a thin membrane is the analog of the load-elongation relationship in a tensile bar. The tension in the membrane is a maximum at the same component of uniaxial strain as the load in the tensile bar. The membrane is unstable if the strain in the membrane exceeds the strain for maximum tension, and the membrane thins down and fractures. A projectile creates a star crack in the membrane at an early stage of the penetration. The concentration of stress at the ends of each branch of the star crack propagates the crack with little expenditure of energy. The plastic energy required for penetration is nearly all absorbed by the petals as they are pushed back from the impact hole. Fracture in a plate of intermediate thickness does not begin until the tip of the projectile has penetrated nearly to the back of the plate.

A homogeneous strain in the medium is unstable with respect to a localized strain wherever the strain in the medium exceeds the strain for maximum shear stress and the medium may rupture by shear[7]. The transition from homogeneous strain to localized strain is probably precipitated by the presence of inhomogeneities in the medium and may be retarded by their absence. The strain in a thick plate exceeds the limiting strain for maximum shear stress everywhere within a zone next to the impact hole. Faults occur within this zone and cracks appear at the surfaces of the plate. The surfaces of the cracks are parallel to the principal plane of shear. Relative motion across each fault produces a concentration of shear strain in the fault, raises the temperature and lowers the shear stress. The material in the fault is quenched after the termination of plastic flow, to a higher hardness than the surrounding medium.

IV THE ELASTIC UNDULATION

The undulation in a thin plate is so wide and shallow that the displacement of the projectile may be represented as the sum of two nearly independent displacements, a displacement ξ of the plate adjacent to the impact hole and a displacement ρ of the projectile with respect to the plate.

The displacement ξ of the plate adjacent to the projectile is assumed in the present analysis to be equal to the displacement at the center of an elastic undulation with the force concentrated at a point. The displacement in an elastic undulation at a distance from the point force would actually be less than the displacement at the point of application, but the displacement in an actual undulation may be greater than the displacement in an elastic undulation because of plastic yielding. The two errors tend to cancel and have therefore been neglected.

There may be a zone of plastic flexure[2] in a plate of intermediate thickness but the zone of plastic flexure is masked in a thin plate by a zone of plastic extension, and is masked in a thick plate by a zone of radial flow from the impact hole.

The momentum delivered to the elastic undulation is not only a function of the displacement ξ at any time, but is also a function of the previous history of the elastic undulation. The momentum is known for two special types of undulation[15]. In the case of a small amplitude of undulation the momentum is directly proportional to ξ, regardless of the variation of force with time, whereas in the case of a large amplitude of undulation, with the force held constant, the momentum is proportional to ξ^2. In the special case of a constant force, the undulation is initially given by the limiting law for small amplitudes, but eventually approaches the limiting law for large amplitudes. The momentum delivered by a constant force may be expressed as a single valued function of the displacement and may be expanded as a power series with constant coefficients. It is assumed in the present analysis that all powers higher than the second may be neglected. The momentum would then be given in the general case by the expression

$$(8.0)\rho\gamma e\xi + (1.09)(\rho E)^{\frac{1}{2}} e\xi^2$$

in which ρ is the density, E is Young's modulus, and γ is a parameter of elasticity. The parameter γ is defined in terms of Young's modulus E and Poisson's ratio σ by the equation

$$\gamma^2 = \frac{e^2 E}{12(1-\sigma^2)\rho}$$

Evidence which supports the validity of this expression for momentum has been found experimentally by the group at the California Institute of Technology[2], who measured the force on a punch which was driven at a constant velocity into the center of a large plate. The force on the punch jumped suddenly to a finite value on contact with the plate, and then increased at a linear rate with time. The square of the initial increment in force should be greater than the rate of

increase in force by a factor equal to

$$\frac{8}{3}\frac{(\rho E)^{\frac{1}{2}}e^3}{(1.09)(1-\sigma^2)}$$

if the equation is valid. The ratio is accurately verified by the experimental results to within the precision of the data.

In the case of a steel plate the parameter γ is given by the equation

$$\frac{\rho\gamma}{e} = (2.48)(10^6)(\text{lb})/(\text{ft})^2(\text{sec})$$

and Young's modulus E is given by the equation

$$(\rho E)^{\frac{1}{2}} = (8.19)(10^6)\ (\text{lb})/(\text{ft})^2(\text{sec})$$

V THE LAW OF FORCE

The relationship between the force on the projectile and the depth of penetration of the projectile into the plate may be derived from the data on the depth of penetration of projectiles into plates at velocities less than limit. The depth of penetration p is measured from the tip of the projectile to a reference plane tangent to the face of the plate just outside of the coronet but inside of the dish. The APL data for the penetration of 3" AP Type A projectiles and 3" AP M79 projectiles into class B armor and STS are given in Figures (5) and (6) where the ratio p/d is plotted against the ratio v_S/v_L. Curves are included in the Figures for even values of e/d, which have been developed through a study of the penetration of service type projectiles of all kinds.

The effect of ogive on the depth of penetration is illustrated by Figure (7), where the APL data for the penetration of 3" AP M79 projectiles into Class B Plate NO. DD37 are compared with the data for 3" AP Type A projectiles. At striking energies near limit the curves for two different nose shapes are nearly parallel and only differ from each other by a constant difference in p. A set of penetration curves have been chosen to represent the 3" AP M79 projectile, and data for curves of constant v_S/v_L are given in Table II where values of p/d are listed for a few values of e/d.

At normal obliquity of the parameter U_S is proportional to the striking energy. A projectile with a small striking energy makes an indentation on the face of a thick plate with a depth of penetration which increases rapidly at first with increase in striking energy. The rate of increase becomes smaller as the striking energy is increased*, until the striking energy is great enough to force the forward bourrelet into the face of the plate. The depth of penetration then increases almost linearly with increase in striking energy, until the nose of the projectile approaches the back of the plate. The penetration then increases more rapidly again with increase in striking energy.

After the striking energy has become large enough to force the bourrelet through the back of the plate, the additional energy required to push the projectile the rest of the way through the plate is only that required to wipe off the rotating band, open any petalling in back which may still be intact, and overcome any frictional resistance which may still be active. The slopes of the curves in Figure (7) therefore approach infinity as the striking energy approaches the limit energy.

The derivative of U_S with respect to p/d is nearly proportional to the force on the projectile, but not quite, because the distance through which the projectile actually moves is greater than the penetration, by the elastic deflection of the plate in the neighborhood of the impact, and because the force is a function of the velocity. The total distance z through which the projectile moves is equal to the sum of the plastic penetration p and the elastic deflection ξ, while the force on the projectile is a function of e/d, p/d and $\dot{z}$. The equation of motion of the projectile may therefore be written

$$\frac{d}{dt}(m\dot{z}) = - f\left(\frac{e}{d}, \frac{z-\xi}{d}, \dot{z}\right) \qquad (1)$$

If the equation of motion be multiplied throughout by $\dot{z}$ and integrated with respect to t, it is replaced by the equation of energy

$$\tfrac{1}{2}mv_S^2 - \tfrac{1}{2}m\dot{z}^2 = \int_o^z f\left(\frac{e}{d}, \frac{z-\xi}{d}, \dot{z}\right)dz \qquad (2)$$

*For example, the penetration of a conical indenter would vary as the cube root of the energy of deformation.

Part of the energy given up by the projectile is stored in the armor adjacent to the point of impact, and part is transmitted to the elastic undulation. If the integration is carried over the whole penetration cycle, the kinetic energy delivered to the armor nearly cancels out, and the integration depends on velocity only through the effect of rate of deformation on the stress, an effect which modifies the integration by a total amount of not more than 2% in the case of an incomplete penetration.

The elastic displacement ξ is a function of the momentum delivered to the elastic undulation. If the whole momentum lost by the projectile is assigned directly to the elastic undulation, then an error is made in ξ, which however vanishes at the end of the penetration cycle, and has relatively little effect on the integration.

In the case of the 3" AP M79 projectile the ratio m/d^3 is equal to 970 (lb)/(ft)^3. For this combination of plate and projectile, the elastic displacement ξ is expressed in terms of the velocity $\dot{z}$ of the projectile by the equation

$$\frac{\xi}{d} = -(1.11)\left(\frac{e}{d}\right) + \sqrt{(1.11)^2\left(\frac{e}{d}\right)^2 + \frac{(0.109)(v_S - \dot{z})}{\left(\frac{e}{d}\right)\ (1000)}} \qquad (3)$$

A set of curves have been developed to represent the steady force on the projectile and are given by solid lines in Figures (8) to (10) where the function $(1/d^2)f$ is plotted against the ratio p/d. The quantity $(1/2)dU_S/d(p/d)$ is also plotted with dotted lines in Figures (8) and (9) for comparison. The shapes of the curves at $v_S/v_L > .8$ were determined by the penetration data, but there are almost no penetration data at $v_S/v_L < .8$. The curves have therefore been so adjusted as to form a family of curves, with an envelope for $e/d = \infty$, which is similar in shape to a plot of the cross-sectional area of the projectile nose contour. The energy per unit volume of indentation for the limiting curve in a plate of infinite thickness would be 440000 (in)(lb)/(in)^3 if there were no coronet formation, whereas the energy per unit volume of indentation in the Brinell hardness test is actually 360000 (in)(lb)/(in)^3 for a steel of 115000 (lb)/(in)^2 tensile strength, and the energy per unit volume of armor in the path of the projectile is only 330000 (in)(lb)/(in)^3 in a plate of caliber thickness.

The force-penetration curves in Figures (8) to (10) for the 3" AP M79 projectile closely resemble the force-displacement curves in Reference (3) for cal. .27 darts, but are more compressed along the axis of the projectile because the ogival radius of the 3" projectile is only 1.67 calibers whereas the ogival radius of the cal. .27 darts was 2.5 calibers.

In the construction of the force-penetration curves, each was adjusted by trial until the function f had the form required by the penetration data. The calculations were based on the equation

$$\tfrac{1}{2}m(v_S^2 - \dot{z}^2) = \int f d\phi + \int f d\xi \qquad (4)$$

which was integrated step by step to find the terminal penetration for each value of v_S. The elastic deflection at each step was obtained from Equation (3).

The force-penetration curves have been integrated for limit impacts at various plate thicknesses. In Table III are given the component parts of $F^2(e/d, \theta)$ which represent the amounts of energy in the elastic undulation and the plastic deformation. The parameter F_S^2 in a complete penetration is given in terms of the component parts F_E^2 and F_P^2 by the equation

$$F_S^2 = F_E^2 + F_P^2 + F_R^2$$

The calculations have been extended to complete penetrations, and are summarized in Table IV where the parameter F_S^2 is tabulated as a function of the parameter F_R^2. Most of the entries in Table IV were obtained by a short cut approximation in which the velocity $\dot{z}$ at any stage of the penetration for a given value of v_R was obtained approximately by quadrature from $\int f d\phi$, and was then used in the calculation of $\int f d\xi$. The approximation was calibrated by step by step integrations for all entries at limit, and for most of the entries for $e/d = 0.25$, and for $e/d = 0.004$. The approximation was corrected throughout by the amount called for by the step by step integrations.

The plastic component F_P^2 is not constant, but increases with increase in impact velocity. At a striking velocity above limit the effect of rate of strain on stress cannot be neglected, and the func-

tion f was therefore replaced in the integration by the expression

$$K\{1 + (.04)\log(\frac{\dot{z}}{v_L})\}f$$

The constant K was so adjusted as to leave the integration unchanged at the limit. The relationship

$$\int f \log(\frac{v_S}{\dot{z}})dz = \frac{1}{2}\int f dz$$

is accurately satisfied by the integrals at limit for all values of e/d, but the factor in the relationship is less than 1/2 at striking velocities greater than limit.

As the striking velocity is increased above limit, the distribution of strain in a thick plate is gradually changed, and the plastic energy for perforation is further increased. The increase in plastic energy is not important in thin plates at impact velocities just above limit, but is significant in plates of thickness greater than half caliber. The absorption functions in Table IV have been so adjusted as to fit the experimental absorption data for plates of thickness greater than half caliber.

The absorption functions in Table IV are plotted with solid lines in Figure (11). Included in the figure are a series of dotted lines of unit slope for comparison which represent the form the absorption functions would have if the energy absorption were constant. Inspection of the figure shows that the slope of the absorption curve at $e/d = 0.65$ is nearly unity, while at e/d less than 0.65 the slopes just above limit are greater than unity, and at e/d greater than 0.65 the slopes are less than unity.

The decrease in slope with increase in e/d was first discovered by Robertson[9] at the Princeton Range where it was interpreted in terms of a Poncelet model of the penetration. That the slopes are consistently greater than one, near limit at e/d less than 0.65, even at normal obliquity, was first discovered by the Armor and Projectile Laboratory, and has since been amply demonstrated by many absorption data. The slopes increase with increase in obliquity, since at high obliquity the projectile is deflected from its original line of flight by an amount which decreases as the striking velocity is increased above limit, and the area of the plate which is subject to plastic deformation becomes smaller. The effect on the absorption curves of increase in obliquity is illustrated by Figure (13).

VI PLATE BOUNDARY EFFECTS

The method of support of a thin plate has an effect on the limit velocity if the elastic undulation reaches the border of the plate before the penetration cycle is complete. The distance R, which the leading edge of the wave has reached at any stage, may be estimated from the volume swept out by the plate during an elastic undulation. In the special case of a constant force f applied to a thin plate of unlimited extent the volume* of the undulation is equal to $(1.11)\xi R^2$, and is also equal in general to the expression[15]

$$\frac{1}{\rho e}\, t \int f dt - \frac{1}{\rho e} \int f t dt$$

The force f in the integration may be replaced approximately by $-m\ddot{x}$ and the integration may be performed by parts. The radius R is then given by the equation

$$R^2 = \frac{m(v_S t - z)}{(1.11)\rho e \xi} \tag{5}$$

It is assumed in the present analysis that this formula is sufficiently accurate under all conditions of practical importance in connection with thin plates.

The method of support of a thick plate has no appreciable effect on the limit velocity unless the plate is so small that the elastic undulation is reflected at the border and returns to the center before the penetration cycle is complete. The fundamental period of vibration of the plate would, in that case, be less than twice the duration of the impact. The fundamental period $(1/\nu)$ of vibration in the case of a square steel plate of side a and thickness e is given by the equation

$$\frac{a^2 \nu}{e} = 15900 \text{ (ft)/(sec)} \tag{6}$$

---

*If the undulation were truly conical the volume would be $\frac{1}{3}\pi\xi R^2$.

Limit determinations with 3" projectiles at the Armor and Projectile Laboratory are made on pieces of armor which are three feet square. The data for plates this size should not deviate by more than a percent from the data for a plate of unlimited extent at any value of ϵ/d greater than 0.25. Either the elastic undulation moves too slowly, or the whole elastic energy is itself too small to have an influence on the limit.

A few shots have been fired at the Armor and Projectile Laboratory against plates with different methods of support, and the data are plotted in Figure (12). The plates were three foot square pieces of modified STS, and were tested with 3" Comm. Mk. 3-7 projectiles at 0° obliquity. The plates were clamped in the butt, or were suspended from wires. Impacts were located at the center of gravity, at a center of percussion* or near a corner. Calculations of the radius R in a limit impact have indicated that the undulation reached the edge of the plate when the elastic energy had reached 93% of its final value in the case of the plate with $\epsilon/d = .083$, and when it had reached 96% of its final value in the case of the plate with $\epsilon/d = .125$. The limit velocities for both plates should therefore deviate by a few percent from the limit for an infinite plate, and the deviation for the thinner plate should be greater than the deviation for the thicker plate. The data for the thinner plate do show some indication that the limits for the free suspension are greater than the limits for the clamped suspension, whereas the data for the thicker plate do not. Dotted curves are included in the figure to illustrate the effect on the absorption curve of a shift from clamped suspension to free suspension in the case of a perfectly rigid plate. A free rigid plate of mass m' would retain after impact a velocity v'_R which satisfies the equation of momentum

$$mv_S = mv_R + m'v'_R$$

The kinetic energy of the projectile is given by the equation

$$\tfrac{1}{2}mv_S^2 = \tfrac{1}{2}mv_R^2 + \tfrac{1}{2}m'v_R'^2 + \tfrac{1}{2}mv_L^2$$

in which $(1/2)mv_L^2$ is the limit energy for a clamped rigid plate.

---

*The center of percussion was a point on a median line at a distance from the center equal to one third the distance from center to edge.

VII EQUILIBRIUM FLOW

Bethe's Theory

The projectile exerts a stress on the plate which is normal to the surface of contact between the plate and the projectile. The force on any element of the surface has, therefore, a radial component as well as an axial component. The ratio between the two components of force depends upon the taper of the projectile nose contour. The axial component of force becomes smaller as the taper of the nose is made less. The displacement in the elastic undulation however does not, at the same time, increase indefinitely, but is limited by the finite limit velocity for penetration. The energy in the elastic undulation is therefore zero and the energy of penetration is primarily plastic in the limit as the taper goes to zero.

An elementary theory has been given by Bethe[6] for the limiting case as the taper goes to zero and the thickness of the plate goes to zero. It is assumed by Bethe that the final energy required to make a given hole in the plate is essentially the same, regardless of the mechanism of the penetration cycle. The idealized theory is thus assumed to be valid for a real projectile.

It is assumed in Bethe's theory that the medium almost obeys the Mohr criterion of plastic yielding. A medium which exactly obeyed the Mohr criterion with constant stress differences would be unstable. A precise comparison between Bethe's theory and the results of ballistic test would not be possible because the stress differences in any actual medium are not constant. Bethe's theory may be modified, however, to include the effects of work hardening.

Equilibrium Expansion of a Hole in a Thin Plate with Free Surfaces

It is assumed that the principal axes of stress are everywhere parallel to the central plane of the plate, whereas the principal axes at the free surfaces must actually be parallel to the free surfaces, even though the thickness of the plate is variable. The error introduced by this assumption should decrease with distance from the axis of the hole, however, and the range of validity should increase with decrease in the thickness of the plate.

Motion in the plate is governed by the equation of equilibrium

$$\frac{d}{dr}(reX_1) = eX_2 \tag{7}$$

in which r is the radial distance from the axis of the hole, e is the variable thickness of the plate, and X_1 and X_2 are the radial and circumferential components of stress. The axial component of stress is zero. A point in the medium which was initially at the distance λ from the axis is displaced by deformation to the distance r. It is assumed that the medium is incompressible, and the invariance of volume is expressed by the equation

$$\pi\lambda^2 = 2\pi\int_{\frac{d}{2}}^{r} erdr \tag{8}$$

There exists a particular solution of the equations, in which the ratio r/d is a stationary function of the ratio λ/d. This solution represents a deformation whose radial dimensions increase uniformly in scale as the impact hole slowly expands. The components of strain, and the components of rate of strain may all be expressed in terms of the stationary function and the rate of expansion. The octahedral shear stress in the medium is a known function of the octahedral shear strain and the ratio between the components of stress. The ratio between the components of stress is a known function of the ratio between the components of rate of strain. The ratio between the components of rate of strain is a function, in turn, of the components of strain, and the second derivative of r with respect to λ, but is independent of the rate of expansion.

The equation of equilibrium and the equation of continuity are integrated simultaneously step by step. The integration is begun at a great distance from the impact hole where the deformation is elastic and the properties of the medium are known exactly. The second derivative of r with respect to λ is known at any step. It is integrated forward one step to give new values for r, the first derivative of r, the components of strain, the octahedral shear strain and the octahedral shear stress, which are all computed in that order. The derivative of X_1 with respect to λ is known at any step. It is integrated forward one step to give new values for the components of stress, the ratio between the components of stress, the ratio between the rates of strain, the second derivative of r with respect to λ and the derivative of X_1 with respect to λ. This completes the step, and the next step may then be begun. The integration is continued until λ is zero.

In the special case of an incompressible medium, the deformation is a pure shear. The stress differences are all proportional to the octahedral shear stress and the equation of equilibrium becomes

$$X_1 = \sqrt{6} \int \frac{1}{r} \frac{1}{3} \sqrt{\Sigma (X_m - X_n)^2}\, dr \qquad (11)$$

The equation of continuity may be integrated at once to give the principal components of strain, the octahedral shear strain, and the octahedral shear stress. The principal components of stress may then be calculated by quadrature.

In the general case of a compressible medium, the mean hydrostatic tension in the incompressible medium may be substituted into the equation of continuity for a compressible medium to give approximately the deformation in the compressible medium.

The energy required to expand the hole in the plate is equal to the product of the volume of the hole and the radial component of stress at the surface of the hole.

The integration has been completed for STS of 115000 $(lb)/(in)^2$ tensile strength. In a compressible medium the plastic energy is slightly less than it is in an incompressible medium. Compression in the medium lowers the plastic energy by 3%. Shear stress in the medium is raised by the application of isotropic pressure at the rate of 6% increase in stress per 100,000 $(lb)/(in)^2$ increase in pressure. This effect alone raises the plastic energy by 8.5%. The plastic energy in an adiabatic deformation would be 3% less than the plastic energy in an isothermal deformation if the strain were uniformly distributed, and would be a few percent lower yet in the presence of faults.

If the medium were perfectly homogeneous, the plastic energy for an isothermal radial expansion would contribute to $F^2(e/d, \theta)$ the component

$$F_p^2 = (30.8)(10^8)$$

but in an adiabatic expansion, with fault formation, the component might be as small as

$$F_p^2 = (27.9)(10^8)$$

The integration has been completed for STS of 115000 (lb)/(in)^2 tensile strength. The actual isothermal stress-strain-rate of strain relationships were used until the interaction between the variables became too difficult to control. The integration was completed with a simplified stress-strain curve which joined the actual stress-strain curve with the same ordinate and slope, but was independent of the ratio between the stresses. Detailed integration cannot be carried all the way to the surface of the impact hole, since the strain becomes infinite. The energy of deformation approaches a constant limit, however, which may be found by an obvious extrapolation.

At a great distance from the impact hole the deformation is pure shear, in an intermediate zone the deformation is approximately a compression, and at the surface of the hole the deformation is approximately a shear again.

If the medium were perfectly homogeneous, the plastic energy for the slow expansion of a hole in a plate would contribute to $F^2(e/d, \theta)$ a component equal to

$$F_p^2 = (19.8)(10^8)$$

The actual medium cannot sustain an infinite strain however without failure, and the actual plastic energy would be a few percent less.

Equilibrium Radial Expansion of a Hole in a Thick Plate with Constrained Surfaces

If the medium is constrained to move radially, the principal axes of stress and strain are truly parallel to the central plane. The equation of equilibrium between the principal components of stress is reduced to the equation

$$\frac{\partial X_1}{\partial r} + \frac{1}{r}(X_1 - X_2) = 0 \qquad (9)$$

and the equation of continuity is reduced to the equation

$$r^2 = 2\int(1 + \frac{1}{\varkappa}\frac{1}{3}\Sigma X_m)\lambda d\lambda \qquad (10)$$

in which $\varkappa$ is the bulk modulus and $\frac{1}{3}\Sigma X_m$ is the mean hydrostatic tension.

Static Indentation Hardness Tests

The static penetration of a conical indenter into a block of hardened copper has been investigated by the group at the University of Cambridge[5]. The energy per unit volume of indentation was found to be constant, as the cone entered the block, until the shoulder of the indenter entered the face of the block. The energy per unit volume of indentation then increased slowly to nearly twice its initial value. The surface of the block was elevated into a coronet during the early stages of the penetration, but the flow in the block was primarily radial near the end of a deep penetration. The energy per unit volume of indentation was lowered by more than one third when the indenter was rotated or lubricated to reduce friction, and the elevation of the coronet was increased.

Projectile Impact

Equilibrium flow in a projectile impact is limited to a zone next to the surface of the plate where one component of stress is maintained zero by the transverse waves. It is assumed in the present analysis that the plastic energy per unit volume of displaced medium is the same, at the surface of the plate, as the plastic energy per unit volume of displaced medium at an expanding hole in a thin plate with free surfaces.

VIII IRROTATIONAL FLOW

The Velocity Potential

If the velocity of propagation of transverse waves were everywhere zero, the flow in the medium would be irrotational.

Irrotational flow in a plate is governed by a velocity potential ψ which is nearly zero at the free surfaces of the plate, where the pressure is zero, but varies with time in the interior of the plate. The velocity potential ψ at any point is a solution of Laplace's equation

$$\nabla \cdot \nabla \psi = 0 \tag{12}$$

or the equivalent integral equation

$$\psi = \frac{1}{4\pi} \int \{ \frac{1}{R} \nabla \psi + \psi \nabla (\frac{1}{R}) \} \cdot ds \tag{13}$$

in which the surface integration is carried over any surface surrounding

the point. The distance R is measured from the surface element ds to the point, and the surface element ds is directed outward from the region occupied by the point.

Irrotational Flow in a Plate

The velocity potential for a projectile in a plate may be represented qualitatively by the potential of a series of positive and negative image nose contours, in addition to the real nose contour, which are arranged symmetrically at equal intervals on each side of the plate. The velocity potential ψ at any point in the medium is given to a first order approximation, by the equation

$$\psi = \frac{1}{4\pi}\int\frac{1}{R}\nabla\psi\cdot ds + \frac{1}{4\pi}\int\psi\, d\omega \qquad (14)$$

in which $\nabla\psi$ is the gradient of ψ at the surface of the nose contour, ds is an element of the surface directed toward the interior of the projectile, R is the distance from the surface element to the point in the medium, and ω is the solid angle subtended by a plane cross section through the nose contour. The integration is carried over the real nose contour and all of its images. The potential at the surface of the nose contour is defined by Equation (14) itself, which is an integral equation of the second kind.

The total displacement of a point in the medium is given approximately by the equation

$$-\int\nabla\psi\, dt = -\frac{1}{4\pi}\iint\nabla\left(\frac{1}{R}\right)\nabla\psi\cdot ds\,dt + \frac{1}{4\pi}\iint\nabla\omega\, d\psi\, dt \qquad (15)$$

The first term in Equation (15) is analogous to the field of a series of cylinders of uniform source density which alternate in sign from one cylinder to the next, while the second term is analogous to the field of a series of cylinders with a variable source density which is concentrated near the ends of each cylinder. It is assumed in the present analysis that the variation in source density along each cylinder may be neglected.

The total displacement at any point in the medium may then be represented approximately by the field of a series of positive and negative uniform cylinders whose source density is so adjusted as to bring the total volume of displaced medium into equality with the medium originally located within the boundaries of the impact hole.*

*A more accurate analysis[18] of the potential, with an approximate allowance for the deformation of the surfaces of the plate, leads to essentially the same displacements.

The potential for a series of positive and negative coaxial cylinders of uniform source density may be found directly from Laplace's equation, of which the potential is one solution. The potential is expressed as an infinite series of terms which contain Hankel functions.

Any point on the free surface of the plate is displaced in a direction nearly normal to the free surface, but a point on the central plane of the plate is displaced in a radial direction. That portion of the surface of the plate which was in the path of the projectile before impact is spread out during impact and becomes the lining of the impact hole.

The contour into which the free surface of a plate of caliber thickness would be deformed by irrotational flow is compared in Figure (14), with the contours for irrotational flow in plates of other thicknesses.

Irrotational flow in the plate produces nearly pure shear at a great distance from the impact hole, with the principal axes of strain in the same plane as the axis of symmetry. At the free surfaces of the plate the principal axes of strain are at 45° to the free surfaces, but on the central plane the principal axes of strain are at 0° to the central plane. Near the impact hole the strain is more nearly pure compression. Although the principal axes of strain vary in orientation through the thickness of the plate, the octahedral shear strain for irrotational flow is nearly constant through the plate.

The plastic energy of deformation per unit thickness at the surface of the plate may be found directly from the contour of the surface. The octahedral shear strain at the surface is related to the rate of change of thickness with distance from the axis by the equation

$$\frac{1}{3}\sqrt{\Sigma(e_m-e_n)^2} = \frac{1}{\sqrt{6}}\frac{de}{dr} \qquad (16)$$

in which $\frac{1}{3}\sqrt{\Sigma(e_m-e_n)^2}$ is the octahedral shear strain, e is the thickness of the plate and r is the radial distance from the axis of the hole. The energy density may be found in terms of the octahedral shear strain by integration of the work done on unit volume along the stress strain curve for pure shear at zero pressure.

The integration has been completed for STS of 115000 $(lb)/(in)^2$ tensile strength. The plastic energy for an adiabatic deformation in a plate of caliber thickness would be 6% less than the plastic energy for an isothermal deformation if there were no faults, but might be 22% smaller yet as the result of fault formation.

If the medium were perfectly homogeneous, the plastic energy per unit thickness at the surface of a plate of caliber thickness would contribute to $F^2(e/d, \theta)$ the component

$$F_p^2 = (26.3)(10^8)$$

in an isothermal, irrotational expansion, but the component might be as small as

$$F_p^2 = (19.3)(10^8)$$

in a slow adiabatic expansion with fault formation.

If the medium were perfectly homogeneous, the plastic energy per unit thickness at the surface of a plate of infinite thickness would contribute to $F^2(e/d, \theta)$ the component

$$F_p^2 = (26.8)(10^8)$$

in an isothermal, irrotational expansion, but the component might be as small as

$$F_p^2 = (25.6)(10^8)$$

in a slow adiabatic expansion with fault formation.

The plastic components of $F^2(e/d, \theta)$ for a few other plate thicknesses are given in Table VIII.

As a cylinder of constant source density is tilted to an angle of obliquity, the total strength of the cylinder is increased by a factor which is inversely proportional to the cosine of the angle of obliquity. The potential of the tilted cylinder differs from the potential of an upright cylinder with the same density and total strength, by terms which vary with azimuth angle, and average out to zero. The plastic energy per unit volume of armor in the plate of a projectile of diameter d in an oblique impact at obliquity θ should therefore be the same as the plastic energy per unit volume of armor in the path of a projectile which has a larger diameter $d/(\cos^{\frac{1}{2}}\theta)$ and strikes the plate at normal obliquity. An obliquity function θ which is based on such a relationship is represented by Curve II in Figure (4) where it is compared with an obliquity function of ballistic origin.

Irrotational Flow in an Infinite Medium

The flow around a projectile nose contour of conventional design may be represented approximately by the flow from a continuous distribution of sources along the axis.

The special case of a point source corresponds to the flow around a nose contour, which is similar in appearance to the nose contours of modern round nosed projectiles. The strength Q of the source is given by the equation

$$Q = \tfrac{1}{4}\pi d^2 \dot{z} \tag{17}$$

in which $\dot{z}$ is the velocity of the source. The particle velocity v in an incompressible medium at a distance R from the source is given by the expression

$$v = \frac{Q}{4\pi R^2} \nabla R \tag{18}$$

in which ∇R is a unit vector directed away from the point source. The velocity in the medium is equal but opposite to the gradient of a scalar velocity potential ψ, which is given by the equation

$$\psi = \frac{Q}{4\pi R} \tag{19}$$

The nose contour is the surface into which any plane in the medium, normal to the axis, is eventually deformed by flow. The equation for the nose contour is

$$\frac{z}{d} = \frac{\left(\frac{1}{4} - 2\frac{r^2}{d^2}\right)}{\sqrt{1 - 4\frac{r^2}{d^2}}} \tag{20}$$

in which r, z are the cylindrical polar coordinates of a point on the nose contour. The distance r is measured radially from the axis of the nose and z is measured axially from the point source.

Kinetic energy is carried forward in the medium around the nose contour. The kinetic energy is equal to $\frac{1}{48}\pi\rho d^3 \dot{z}^2$, which is just one fourth of the kinetic energy of a sphere of the medium with a diameter of one caliber, and is one half of the kinetic energy in the medium surrounding a sphere in a perfect fluid.

The Bernoullian pressure in the medium is a maximum at the tip of the nose contour, where it is equal to $\frac{1}{2}\rho\dot{z}^2$, and is a minimum near the sides of the nose contour, where it is equal to $-\frac{1}{8}\rho\dot{z}^2$.

Exact analytic expressions may be found for the deformation at any point in the medium. The rate of strain at any point is pure compression, with a uniaxial component equal to

$$-\frac{Q}{2\pi R^3}$$

The axes of strain rate at a point in the medium rotate through an angle of almost 180° as the source goes by. The strain in the medium is a compression at a point in advance of the source, but is more nearly a shear at a point in the rear of the source. The components of strain may be expressed in terms of elliptic integrals. Any sphere in the medium is transformed by deformation into an ellipsoid. The axes of the ellipsoid rotate through an angle of almost 90° as the source goes by.

Work is done on unit volume of the medium at a rate equal to the sum of the products of the components of stress and the components of strain rate. The sum of the components of strain rate is zero, and two components of stress are equal. Work is therefore done on unit volume at a rate equal to the product of the uniaxial component of strain rate and the common difference in stress. The stress difference is given by the expression

$$\frac{3}{\sqrt{2}}\frac{1}{3}\sqrt{\Sigma(X_m-X_n)^2}$$

in which $\frac{1}{3}\sqrt{\Sigma(X_m-X_n)^2}$ is the octahedral shear stress. Work is done on the whole medium at a rate $\dot{w}$ which is given by the equation

$$\dot{w} = Q\iint \frac{1}{\sqrt{2}}\sqrt{\Sigma(X_m-X_n)^2}\,\frac{1}{R}\sin\theta\,dR\,d\theta \qquad (21)$$

in which R,θ are spherical polar coordinates. The distance R is measured from the point source to a point whose polar angle is θ. The integration may be performed without a complete knowledge of the distribution of stress, since the octahedral shear stress is a function only of the octahedral shear strain and the components of rate of strain.

The rate of doing work has been computed for a point source in STS of 115000 (lb)/(in)^2 tensile strength. If the medium were perfectly homogeneous, the plastic energy for isothermal irrotational flow would

contribute to $F^2(e/d,\theta)$ a component equal to

$$F_p^2 = (58.8)(10^8)$$

but the component for a slow adiabatic flow with fault formation might be as small as

$$F_p^2 = (51.0)(10^8)$$

The plastic energy near a source which is moving rapidly through STS with the velocity $\dot{z}$ would be greater than the energy near a slowly moving source by the factor

$$(1.20)\{1 + (.04)\log(\frac{\dot{z}}{1000d})\}$$

in which the velocity $\dot{z}$ must be expressed in (ft)/(sec) and the diameter d in (ft).

The general case of irrotational flow around an arbitrary nose contour may be represented approximately by a linear source density, or strength per unit length along the axis of symmetry which varies from point to point along the axis. The total flux $Q(\alpha)$, which is flowing from all of the sources with coordinates greater than α, is given by the equation

$$Q(\alpha) = \int_{\alpha}^{\infty} q(\alpha)d\alpha$$

in which $q(\alpha)$ is the linear source density. The function $Q(\alpha)$ is defined by the continuity of flux across any section of the nose contour. It is a solution of the equation

$$\pi r^2 = \frac{1}{2}\int_{-\infty}^{+\infty} \frac{r^2}{(r^2 + (\alpha-z)^2)^{\frac{3}{2}}} Q(\alpha)d\alpha \qquad (22)$$

in which r,z are the cylindrical polar coordinates of a point on the nose contour. The equation is an integral equation of the first kind with an unsymmetric kernel, but may be transformed into an integral equation with a symmetric kernel, and may be solved by methods of successive approximations. Accurate general formulae may be derived which express the velocity potential, the deformation contours and stream lines, the components of strain rate and the components of strain in terms of $Q(\alpha)$.

The integration has been completed for a 3" AP M79 projectile nose contour. The kinetic energy which is carried forward in the medium around the projectile nose contour is equal to $(.0206)\pi\rho d^3\dot{z}^2$, and is 1% less than the energy near a point source. The kinetic energy in steel is only 6.5% of the kinetic energy of the standard 15 lb. projectile. The Bernoullian pressure at the tip of the projectile is still $\frac{1}{2}\rho\dot{z}^2$, but has a minimum value along the sides of the contour, equal to $-(.171)\rho\dot{z}^2$.

The strain rate in the medium is pure compression on the axis ahead of the projectile, but differs from pure compression at other points, and approaches pure shear at a point on the surface of the projectile in the rear of the bourrelet. The components of strain rate, the components of stress and the rate of doing work may be calculated in turn from the velocity potential and the octahedral shear strain. The rate of doing work has been computed for a 3" AP M79 projectile in STS of 115000 $(lb)/(in)^2$ tensile strength. If the medium were perfectly homogeneous, the plastic energy for isothermal irrotational flow would contribute to $F^2(e/d,\theta)$ a component equal to

$$F_p^2 = (60.2)(10^8)$$

but the component for a slow adiabatic flow with fault formation might be as small as

$$F_p^2 = (54.3)(10^8)$$

The plastic energy near a projectile which is moving rapidly through STS with the velocity $\dot{z}$ would be greater than the energy near a slowly moving projectile by the factor

$$(1.18)\{1 + (.04)\log(\frac{\dot{z}}{1000d})\}$$

in which the velocity $\dot{z}$ must be expressed in (ft)/(sec) and the diameter d in (ft).

The plastic energy near a 3" AP M79 projectile in an infinite medium is greater than the plastic energy in a pure radial expansion by a ratio of 1.95, even though the final distribution of strain is nearly the same in both. The additional energy is the result of rotation of the principal axes of strain rate at each point in the medium as the deformation progresses. The rotation of axes of strain rate produces the same final strain, but involves a greater amount of plastic work.

The plastic energy in a plate of finite thickness is also greater than the plastic energy for the same final strain with fixed axes of strain rate by a smaller ratio which approaches unity as the thickness of the plate is decreased. In the case of a 3" AP M79 projectile in a plate of caliber thickness the ratio is only 1.14. The estimated ratio for other thicknesses is listed in Table VII.

IX THIN PLATE THEORY

The undulation in the elastic zone advances to a distance of many calibers from the point of impact while a projectile is penetrating a membrane at normal obliquity. The radius of the leading edge, at any stage of the penetration cycle, becomes greater as the thickness of the membrane is made less. The undulation in the plastic zone is propagated with a velocity which is nearly constant and much greater than the velocity of the projectile. The plate is therefore in equilibrium near the point of impact in the limiting case of a thin membrane, and wave propagation is only important at the outer edge of the elastic undulation.

The radius of the plastic zone is determined by the conditions for equilibrium, and is given in terms of the yield stress Y' by the expression[18]

$$\frac{3}{64}\sqrt{3}\left(\frac{E}{Y'}\right)^{\frac{1}{2}}\frac{6f}{2\pi Y' e}$$

The radius of the plastic zone steadily increases during the penetration as the force on the membrane increases. The final radius of the plastic zone is limited by the maximum force on the membrane during penetration. The radius of the elastic undulation continues to increase even after the force has passed the maximum, but the radius of the plastic zone does not.

In the case of STS with a tensile strength of 115000 (lb)/(in)^2, the velocity of propagation of an undulation in the plastic zone is 1040 (ft)/(sec). The radii of the elastic and plastic zones have been calculated for the penetration of a 3" AP M79 projectile at normal obliquity. The radius of the elastic undulation at the instant when penetration is half complete is listed for a few values of e/d in Table V, together with the maximum radius of the plastic zone. The membrane is under biaxial tension at the tip of the projectile. The stress-strain relationship for biaxial tension is nearly identical in form to the stress-strain relationship in the conventional tensile test, since two components of strain are equal in both cases. The strain normal to the membrane in biaxial tension is the analog of the strain along the axis in the tensile

test. The tension in the membrane is equal to the product of the stress in the membrane and the thickness of the membrane, whereas the load in the tensile test is equal to the product of the stress in the specimen and the area of the specimen. The ratio between tension and load is nearly constant for the same amount of uniaxial strain. The tension in the membrane passes through a maximum, at the same stress as the load in the tensile test, but the biaxial strain at the maximum is half the uniaxial strain.

If the strain in the membrane exceeds the strain for maximum tension, the membrane thins down by contraction through its thickness, since it is not free to contract in a transverse direction parallel to its surface.

A pointed projectile creates a star crack in a membrane almost at the instant of contact, and a round nosed projectile creates a star crack shortly after the instant of contact. The energy expended on the petals of an n-petal star crack contributes to $F^2(e/d,\theta)$ an amount F_p^2 which is given by the equation[16]

$$F_p^2 = \frac{\pi}{n^2} X' \tag{23}$$

The yield stress X' in the equation is best represented numerically by the dynamic tensile strength for the prevailing rate of strain.

An attempt has been made to determine experimentally the limit approached by $F(e/d,\theta)$ as e/d goes to zero. An uncapped 3" AP Type A projectile was dropped from various heights on pieces of .011" sheet steel of 46000 (lb)/(in)^2 tensile strength. The experimental value of $F(e/d,\theta)$ was 10100±100. The pieces were only two feet square in size, and were crimped between two tightly fitting wooden frames, which left an unsupported square surface of sheet steel only 18" on a side. Calculation of the radius of the elastic undulation indicates that the leading edge of the undulation had already reached the edge of the sheet when the elastic energy was still only 6% of its final value. It is evident therefore that the elastic undulation was nearly suppressed, and the energy of penetration was nearly all plastic. In order to perform the experiment properly the sheet would have to be at least 15 ft. square.

The dynamic tensile strength of this sheet steel is not known, but should be somewhere near the dynamic tensile strength for mild steel. The prevailing strain rate was at least 20 (sec^{-1}), and the dynamic tensile strength for this strain rate should be 62000±2000 (lb)/(in)^2. The number of petals in each star crack was three. The corresponding

theoretical value for $F(e/d, \theta)$ is 10000±200, which is near enough to the experimental value to indicate that the theory is at least qualitatively correct. The plastic energy required for the penetration of STS should be greater than the penetration energy for these sheets of steel, and might be as large as the entries at the bottom of Table III, which are greater than the values for sheet steel by the ratio between the dynamic tensile strength of the two materials.

That the biaxial strain cannot exceed the strain for maximum tension except at a crack was verified experimentally during the tests with sheet steel. Two circles were scribed on one of the sheets with a compass. The circles were initially separated by a small but uniform difference in radius. The projectile was then allowed to fall on the sheet with just enough velocity to crack the sheet. The separation between the circles was increased by 10% at the tip of the projectile, whereas maximum load in the tensile test occurred at an elongation of 21%.

As the plate is increased in thickness, and offers more resistance to penetration, the projectile must penetrate through a greater thickness of plate before the strain at the back of the plate reaches the strain for maximum tension. Plastic energy is therefore delivered to a thin plate of finite thickness prior to the formation of a star crack.

The plastic energy is essentially that energy which is required to bring the tip of the projectile just to the back of the plate. The projectile is then in contact with the plate over a surface which extends back from the tip to a distance greater than the thickness of the plate. The pressure applied to the projectile over the surface of contact is of the same order of magnitude as the tensile strength of the plate material. The plastic energy is essentially equal to the product of the average pressure and the volume of the imbedded portion of the nose contour. The total plastic energy required for penetration is equal to the sum of the energy required to crack the plate and the energy required to bend back the petals after fracture.

Theoretical plate penetration coefficients for 3" AP M79 projectiles vs. thin STS of 115000 $(lb)/(in)^2$ tensile strength have been calculated, and the results are compared with the test data in Figure (2). The average stress on the projectile was assumed to be the same as the average stress at the surface of an expanding hole of uniform diameter. For a slow expansion the average stress would be 105000 $(lb)/(in)^2$, but for dynamic conditions of deformation the stress was assumed to be greater by the ratio between the dynamic and static tensile strengths. The prevailing strain rate before fracture is of the order of 200 $(sec)^{-1}$, and for this strain rate the tensile strength for STS should be

145000±5000 (lb)/(in)^2. The thickness of each lamina of the plate was assumed to be the same, at the surface of the impact hole, as the thickness at the surface of an expanding hole of uniform diameter. The imbedded portion of the nose contour was therefore assumed to extend back from the tip to a distance equal to (2.6)e at the instant of fracture. The theoretical curve in Figure (2) is lower than the experimental curve, but agrees with it to within the precision of either.

The energy required to push back the petals is assumed in the present theory to be all expended on distortion of the perimeter of the petal, whereas a small additional component of energy is required to bend the surface of the petal.[12] The bending energy in a thin plate which is already subject to extension as well as flexure increases with increase in plate thickness, but is only a small quantity of the second order. The number of petals in the star crack is assumed to be constant, whereas the actual number of petals tends to increase with increase in plate thickness. The two effects tend to cancel, and have therefore been neglected.

X THICK PLATE THEORY

A surface in the medium which was originally cylindrical and concentric with the axis would be deformed by irrotational flow into a new surface which is convex outward, whereas the surface would be deformed by rotational flow into a new surface which is concave outward.

Pure irrotational flow in an actual plate of plastic material is limited to a zone on the central plane of the plate and adjacent to the impact hole. Outside of the zone the deformation is rotational. This is illustrated in Figure (17) which represents the actual deformation contours in a limit impact. Near the center of the plate and near the impact hole the deformation contours are similar to the contours generated by irrotational flow, but at the free surfaces of the plate the contours are perpendicular to the free surfaces and the deformation is rotational. The theoretical boundary of the zone of irrotational flow is outlined in Figure (16), by the leading edge of a distortional wave which is propagated inward from the surface for a period of d milliseconds. It was assumed in the analysis that the strain increases to its final value at a constant rate in the same period of time. The strain in an actual limit impact increases at approximately this rate. The zones of irrotational flow in Figures (16) and (17) are essentially the same. The zone of rotational flow in the actual impact is narrower at the face of the plate, where the projectile is moving rapidly, than it is at the back of the plate, where the projectile comes to a stop. The depth to which a transverse wave penetrates a face of the plate is proportional to the time

which the projectile spends in the neighborhood of the face. If the projectile were pushed slowly through the plate, the transverse waves would have time to maintain more of the medium in a state of equilibrium and the deformation would approach the theory of equilibrium flow; but if the projectile struck the plate at a high velocity above limit, the deformation would be better represented by the theory of irrotational flow.

The length of the deformation contour for a particular volume of inscribed medium is greatest when the flow is irrotational and least when the flow is rotational. The length in an actual deformation at limit is nearly the same as it would be if the cylindrical surface remained a cylinder.

Theoretical contours of the free surface for the two limiting types of flow are compared in Figure (15) for a plate of caliber thickness. If the flow were irrotational, the elevation* of the plate at the impact hole would be nearly independent of plate thickness and would be equal to $(.38)d$, but if the medium were in equilibrium the elevation might be twice as large. The mean elevation at the front and back of actual impact holes have been found experimentally[3] to vary from $(.4)d$ to $(.5)d$ as e/d varied from .7 to 1.9. The elevation of the plate near the impact hole is therefore nearly given by the theory of irrotational flow. At a distance from the impact hole however, the elevation for irrotational flow is greater than the elevation for equilibrium flow.

If the flow were irrotational, the elevation at a distance of 2.05 calibers from the point of impact would be $(.03)d$ in a plate 4 calibers thick, but has been found experimentally[4] to be less than $(.001)d$. The elevation for equilibrium flow at this distance would be $(.0003)d$. The elevation of the plate far from the impact hole is therefore nearly given by the theory of equilibrium flow, a result which is confirmed by the shape of the experimental contour in Figure (17).

Theoretical values for $F^2(e/d, \theta)$ have been calculated for the 3" AP M79 projectile and are listed in Table IX for a few plate thicknesses. The plastic energy was calculated first for the limiting case of equilibrium flow, then also for the limiting case of irrotational flow. The actual energy is intermediate between these

*A theoretical formula[11] for the elevation at the point of impact has been given by G. I. Taylor, "Notes on Bethe's Theory of Armor Penetration", British Report R.C. 280. Taylor's formula gives an elevation which increases with thickness at a faster rate than in direct proportion to thickness, whereas the contrary is found experimentally.

two values. The energy density at each point in the medium was first calculated from the components of strain for a deformation with the principal axes of strain rate and the principal components of strain rate all held constant*. To this energy were then added corrections for the rotation of the principal axes of strain rate, and for the increase in stress with increase in strain rate.

The plastic energy at the surface of a plate of caliber thickness, in the limiting case of equilibrium flow, would contribute to $F^2(e/d,\theta)$ the component

$$F_p^2 = (20.8)(10^8)$$

in an isothermal deformation with stationary principal axes of strain rate, but the component might be as small as

$$F_p^2 = (15.1)(10^8)$$

in a slow adiabatic deformation with fault formation.

The plastic energy in a plate of caliber thickness, in the limiting case of irrotational flow, would contribute to $F^2(e/d,\theta)$ the component

$$F_p^2 = (26.3)(10^8)$$

in an isothermal deformation with stationary principal axes of strain rate, but the component might be as small as

$$F_p^2 = (19.3)(10^8)$$

in a slow adiabatic deformation with fault formation. The most likely value for the plastic component of $F^2(e/d,\theta)$ is intermediate between the two values for adiabatic flow with fault formation. The relative amounts of energy which may be assigned to irrotational flow and to equilibrium flow may be estimated in terms of the duration of irrotational flow at each point in the medium. In the central zone of Figure (16) the flow is entirely irrotational, just outside of the central zone the flow is

---

*The validity of the assumption that the components of strain rate may be held in a constant ratio was tested by comparative calculations of the plastic energy in the case of equilibrium flow. The approximation was too small by only 0.6%.

partly irrotational and partly at equilibrium, while at a distance from the impact hole the medium is essentially at equilibrium. The energy in each element of volume has been multiplied by the duration of irrotational flow and the product has been integrated over the whole volume of medium, to find that fraction of the plastic energy which may be assigned to irrotational flow. The fraction has been found to be approximately one half. The most likely value for the plastic component of $F^2(e/d, \theta)$ in a plate of caliber thickness is therefore

$$F_p^2 = (17.2)(10^8)$$

in a slow adiabatic deformation with stationary principal axes of strain rate.

The same component has been found by calculation in the simplified case of a plastic deformation in a plate with cylindrical internal deformation contours, but with the external surface for irrotation flow.

It is assumed for the purposes of the present analysis, that the relative amounts of energy, to be assigned to equilibrium flow and to irrotational flow, are also in the same ratio, for plates of thicknesses greater than one caliber.

The principal axes of strain rate rotate with respect to the medium only in the interior of the medium. In the central zone next to the impact hole the energy density is raised by rotation of the principal axes of strain rate to nearly the full amount for pure irrotational flow, but the energy density is not raised at all at the free surfaces, and is raised to an intermediate amount at other points in the medium. Rotation of the principal axes of strain rate modifies only that part of the plastic energy which may be assigned to irrotational flow. The plastic component of $F^2(e/d, \theta)$ in a plate of caliber thickness is raised to the value

$$F_p^2 = (18.6)(10^8)$$

by rotation of the principal axes of strain rate.

The dynamic pressure in the medium raises the shear stress and increases the plastic energy by a small amount which is negligible in a plate of caliber thickness, but amounts to a few percent in plates of greater thickness.

The strain rate in the medium varies with time as the projectile passes through the plate, and varies from point to point in the plate. The plastic energy for rapid deformation is greater than the

plastic energy for a slow deformation. It is assumed for the purposes of the present analysis that the fractional increase in plastic energy for a plate of finite thickness is equal, on the average, to the fractional increase in plastic energy for a projectile in an infinite medium*. The plastic component of $F^2(e/d, \theta)$ in a plate of caliber thickness is therefore theoretically equal to

$$F_p^2 = (23.2)(10^8)$$

in the case of rapid adiabatic flow with fault formation near the impact hole. The theoretical and experimental results agree to within the precision of either.

The plastic component of $F^2(e/d, \theta)$ in a plate of caliber thickness would be equal to

$$F_p^2 = (27.6)(10^8)$$

in the case of rapid adiabatic flow without fault formation near the impact hole.

The theoretical values of the plate penetration coefficient in a thick plate are compared with the ballistic data in Figures (2) and (3). Curves are also included in the figures to represent the theoretical plate penetration coefficients for the limiting cases of pure irrotational flow and pure equilibrium flow.

The contour of the free surface for irrotational flow is nearly identical to the contour for equilibrium flow when the plate is half caliber thick, and the zone of irrotational flow in a limit impact is also nearly absent. The theory of thick plates is limited, therefore, to plates of thickness greater than half caliber.

XI ENERGY IN THE COMPRESSION WAVE

As the projectile enters the plate it creates a compression wave and radiates energy[12]. The compression wave is reflected and diffracted at the free surfaces of the plate. The radiated energy does not escape to the borders of the plate, but is converted into energy of vibration. The projectile acts like a source of strength Q, and radiates

*The validity of this assumption has been qualitatively verified by considerations of the rate of strain in a plate of caliber thickness.

energy at a rate given by the expression

$$\frac{\rho Q^2}{4\pi c}$$

in which ρ is the density of the medium and c is the velocity of a longitudinal wave.

The strength Q is equal to the product of the velocity of the projectile and the net cross sectional area of the imbedded portion of the nose contour. The cross sectional area is given qualitatively in terms of the acceleration of the projectile by the equation

$$\tfrac{1}{4}\pi d^2\left(\frac{ef}{\tfrac{1}{2}mv_L^2}\right) = \frac{\tfrac{1}{2}\pi m\ddot{z}}{F^2(e/d,\theta)}$$

The energy in the compression wave contributes to $F^2(e/d,\theta)$ a component part F_C^2 which is given by the equation

$$F_C^2 = \frac{1}{F^2(e/d,\theta)}\,\frac{\pi m\rho}{8c}\,\frac{1}{v_L^2}\int\frac{1}{\dot{z}}\left\{\frac{d}{dt}(\dot{z}\,\ddot{z})\right\}^2 dz \qquad (24)$$

The integration has been completed for a plate of caliber thickness, and the radiated energy has been found to be only 0.3% of the striking energy for a plate of this thickness. The radiated energy varies as the cube of the velocity and becomes, therefore, a larger fraction of the striking energy as the thickness of the plate is increased.

XII CAVITATION

The impact hole has been found experimentally[10,18] to be larger in diameter near the entrance of the hole than it is at the center of the plate. Such an enlargement of the impact hole is at least partly the result of plastic resistance to shear which would cause the lip of the entrance to peel back from the sides of the projectile after the bourrelet had entered the face of the plate. At a sufficiently great velocity of impact the enlargement of the hole should be augmented by cavitation.

The average pressure on the projectile nose in a limit impact is given qualitatively by the expression

$$\frac{\frac{1}{2}mv_L^2}{\frac{1}{4}\pi d^2 e}$$

whereas the cavitation pressure in the case of the 3" AP M79 projectile is given by the expression

$$(.171)\rho v_L^2$$

Cavitation should only be important ballistically in a plate of such thickness that the two pressures are equal. The thickness of an STS plate must be 6 calibers for the two pressures to be equal.

XIII TABLES OF FUNCTIONS

Table I

Relative amount of energy per unit volume of displaced medium for several systems of plastic flow.

System	Energy per unit volume
Equilibrium expansion of a cylindrical hole in a thin plate with free surfaces.	.67
Irrotational flow in a plate of caliber thickness. Consecutive cylindrical sources of alternate sign.	.85
Equilibrium expansion of a cylindrical hole in a thick plate with constrained surfaces. Stationary line source.	1.00
Equilibrium expansion of a spherical cavity. Stationary point source.	1.26
Point Source in motion.	1.91

Table II

The Depth of Penetration of 3" AP M79 Projectiles into Homogeneous Plate

$\frac{p}{d}$

$\frac{v_S}{v_L}$	$\frac{e}{d}$						
	.25	.40	.65	.82	1.00	1.38	1.73
.80	.65	.68	.80	.90	1.02	1.25	1.48
.90	.83	.86	.98	1.09	1.22	1.53	1.82
.95	.99	1.03	1.16	1.28	1.43	1.77	2.09
.98	1.18	1.22	1.39	1.52	1.69	2.05	2.40

Table III

Elastic Energy at Limit for 3" AP M79 Projectile
at 0° Obliquity in STS of 115000 (lb)/(in)^2 Tensile Strength

$\frac{e}{d}$	$(10^{-8})U(\frac{e}{d},\theta)$	v_L	$\frac{\xi}{d}$	$(10^{-8})F_B^2$	$(10^{-8})F_P^2$	$(10^{-8})F^2(\frac{e}{d},\theta)$
1.73	48.4	2236	.036	.4	27.6	28.0
1.38	36.0	1928	.049	.6	25.5	26.1
1.00	24.0	1573	.075	1.0	23.0	24.0
.82	18.9	1396	.097	1.3	21.7	23.0
.65	14.2	1210	.129	1.8	20.0	21.8
.50	10.15	1023	.174	2.4	17.9	20.3
.40	7.44	877	.216	2.7	15.9	18.6
.25	3.33	586	.30	2.7	10.7	13.3
.125	.86	298	.39	1.7	5.2	6.9
.083	.40	203	.43	1.3	3.5	4.8
.05	.19	140	.50	1.1	2.7	3.8
.02	.070	85	.66	1.2	2.3	3.5
.01	.036	61	.80	1.4	2.2	3.6
.004	.0164	41	1.05	1.9	2.2	4.1

Table IV

Absorption Functions for the 3" AP M79 Projectile in STS of 115000 (lb)/(in)^2 Tensile Strength

$(10^{-8})F_S^2$

$\frac{e}{d}$	$(10^{-8})F_R^2$									
	0	1	2	3	5	10	15	20	25	30
1.73	28.0	29.1	30.2	31.4	33.6	39.0	44.4	49.9	55.3	60.7
1.38	26.1	27.2	28.3	29.4	31.5	36.8	42.1	47.4	52.7	58.0
1.00	24.0	25.0	26.1	27.1	29.2	34.4	39.5	44.6	49.8	55.0
.82	23.0	24.0	25.0	26.0	28.0	33.1	38.2	43.3	48.4	53.5
.65	21.8	22.8	23.8	24.7	26.7	31.7	36.7	41.7	46.7	51.7
.50	20.3	21.2	22.2	23.1	25.0	29.9	34.8	39.8	44.7	49.7
.40	18.6	19.5	20.4	21.3	23.2	28.0	32.9	37.8	42.7	47.7
.25	13.3	14.1	15.0	15.9	17.7	22.5	27.4	32.3	37.2	42.2
.125	6.9	7.7	8.6	9.5	11.4	16.3	21.2	26.2	31.2	36.1
.083	4.8	5.7	6.6	7.5	9.4	14.3	19.3	24.2	29.2	34.2
.05	3.8	4.7	5.6	6.5	8.5	13.4	18.3	23.3	28.3	33.3
.02	3.5	4.3	5.2	6.2	8.1	13.0	18.0	32.0	27.9	32.9
.01	3.6	4.4	5.3	6.2	8.1	13.1	18.0	22.9	27.9	32.9
.004	4.1	4.8	5.7	6.6	8.4	13.3	18.2	23.1	28.1	33.1

Table V

The radii of the elastic and plastic zones during the penetration of thin STS by 3" AP M79 projectiles at normal obliquity.

$\frac{e}{d}$	.004	.083	.125
Elastic Radius (calibers)	10	2.9	2.5
Plastic Radius (calibers)	>.42	.63	.85

Table VI

Theoretical values of $F^2(e/d,\theta)$ for a 3" AP M79 projectile in a thin plate of STS with a tensile strength of 115000 (lb)/(in)^2

$\frac{e}{d}$	.004	.01	.02	.05	.083	.125	.25	.40	.50	.65	.82	1.00
$(10^{-8})F^2(\frac{e}{d},\theta)$	4.1	3.6	3.5	3.8	4.7	6.4	12.0	17.3	19.4	21.2	22.3	23.1

Table VII

The estimated fractional increase in plastic energy which may be associated with rotation of the principal axes of strain rate during irrotational flow around a 3" AP M79 projectile

$\frac{e}{d}$	.5	1.0	1.5	2	3	4	5	∞
Ogive Effect	1.01	1.14	1.29	1.41	1.57	1.66	1.71	1.95

Table VIII

Plastic component of $F^2(e/d,\theta)$ for the surface of a plate in the limiting case of slow adiabatic irrotational flow with fault formation near the impact hole.

$\frac{e}{d}$	.5	1.0	1.5	2	3	4	5	∞
$(10^{-8})F_p^2$	15.3	19.3	20.9	21.9	23.2	23.8	24.1	25.6

The plastic component of $F^2(e/d,\theta)$ for the limiting case of slow adiabatic equilibrium flow at the surface of a plate with fault formation near the impact hole is

$$(10^{-8})F_p^2 = 15.1$$

Table IX

Theoretical values of $F^2(e/d,\theta)$ for a 3" AP M79 projectile in a thick plate of STS with a tensile strength of 115000 (lb)/(in)^2. Adiabatic flow with fault formation near the impact hole.

$\frac{e}{d}$	.5	1.0	1.5	2	3	4	5
$(10^{-8})F^2(\frac{e}{d},\theta)$	21.1	24.2	27.2	29.8	33.9	36.2	37.5

XIV REFERENCES

(1) "On the Propagation of Plastic Deformation in Solids", Th. von Karman, NDRC Report No. A-29 (January, 1942).

(2) "The Behavior of Large Plates under Impact Loading", P. E. Duwez, D. S. Clark, D. S. Wood, and D. H. Hyers, NDRC Report No. A-254 (February, 1944).

(3) "The Measurement of Forces which Resist Penetration of STS Armor, Mild Steel, and 24ST Aluminum", G. D. Kinzer, A. V. H. Masket, and J. R. Streeter, NRL Report No. O-2276 (April, 1944).

(4) "Measurement of the Redistribution of Material in Armor upon Perforation," R. J. Emrich, and R. L. Kramer, NDRC Monthly Report OTB-3 (October 15, 1944).

(5) "The Theory of Indentation and Hardness Tests", R. F. Bishop, R. Hill, and N. F. Mott, Proc. Phys. Soc. 57 147 (1945).

(6) "Attempt of a Theory of Armor Penetration," H. A. Bethe, Frankford Arsenal Report of 23 May 1941.

(7) "Mechanism of Armor Penetration, First Partial Report," C. Zener, and J. H. Hollomon, Watertown Arsenal Report No. 710/454 (September, 1942); "Plastic Flow and Rupture of Metals. Second Partial Report", J. H. Hollomon and C. Zener, Watertown Arsenal Report No. 732/10-1 (July, 1943).

(8) "Mechanism of Armor Penetration. Second Partial Report", C. Zener and R. E. Peterson, Watertown Arsenal Report No. 710/492 (May, 1943).

(9) "The Mechanics of Armor Perforation. I Residual Velocity", H. P. Robertson, NDRC Report No. A-16 (July, 1941), H. P. Robertson, A. H. Taub and C. W. Curtis, NDRC Report No. A-227 (November, 1943).

(10) "Cavitation Phenomena in Ductile Materials and the Dynamic Term in the Resistance to Penetration", R. Hill, British Report No. 34/44 (August, 1944).

(11) "Penetration of Armor by High Velocity Projectiles and Munroe Jets", R. Hill, N. F. Mott and D. C. Pack, British Report No. 13-44 (March, 1944).

(12) "Penetration Mechanisms I. The Penetration of Homogeneous Armor by Uncapped Projectiles at 0° Obliquity", NPG Report No. 1-43 (April, 1943).

(13) "Penetration Mechanisms. II. Supplementary Report on the Penetration of Homogeneous Plate by Uncapped Projectiles at 0° Obliquity", NPG Report No. 3-44 (February, 1944).

(14) "Analytical Summary Part I. The Physical Properties of STS under Triaxial Stress", NPG Report No. 6-46 (May, 1946).

(15) "Analytical Summary Part II. Elastic and Plastic Undulations in Armor Plate", NPG Report No. 7-46 (May, 1946).

(16) "Analytical Summary Part III. Plastic Flow in Armor Plate", NPG Report No. 8-46 (May, 1946).

(17) "Ballistic Summary Part I. The Dependence of Limit Velocity on Plate Thickness and Obliquity at Low Obliquity", NPG Report No. 2-46 (March, 1946).

(18) "Ballistic Summary Part II. The Scale Effect and the Ogive Effect", NPG Report No. 4-46 (April, 1946).

NPG PHOTO NO. 2976 (APL) [redacted] FIGURE (1)

THE PLATE PENETRATION COEFFICIENT FOR 0° OBLIQUITY

Standard Experimental Curve for 3" AP M79 Projectile vs STS of 115000 $(lb)/(in)^2$ Tensile Strength at 15°C

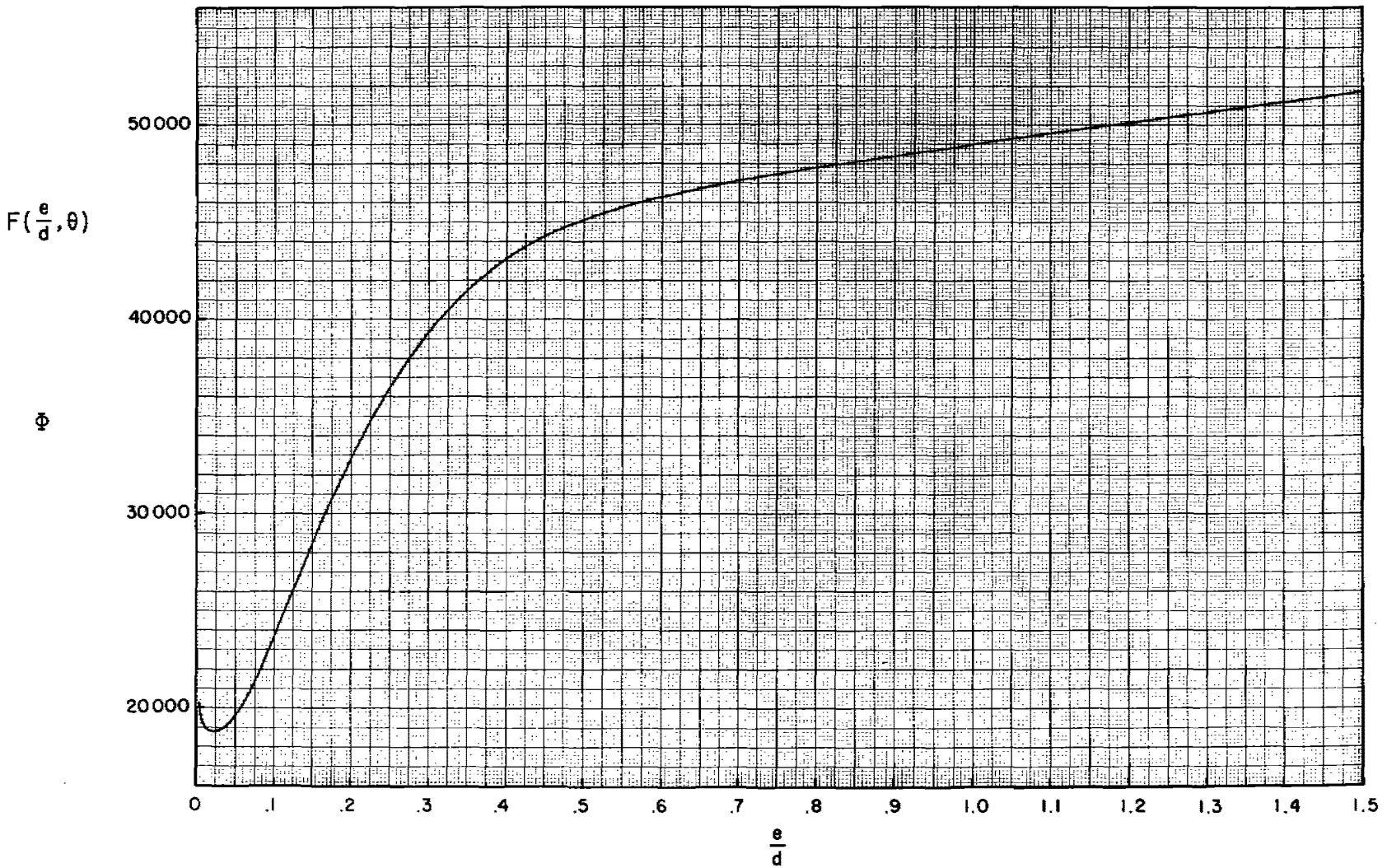

SF

PLATE PENETRATION COEFFICIENTS

Undeformed 3" Monobloc Projectiles vs STS at 0° Obliquity, corrected to 115000 (lb)/(in)^2 Tensile Strength and 15°C

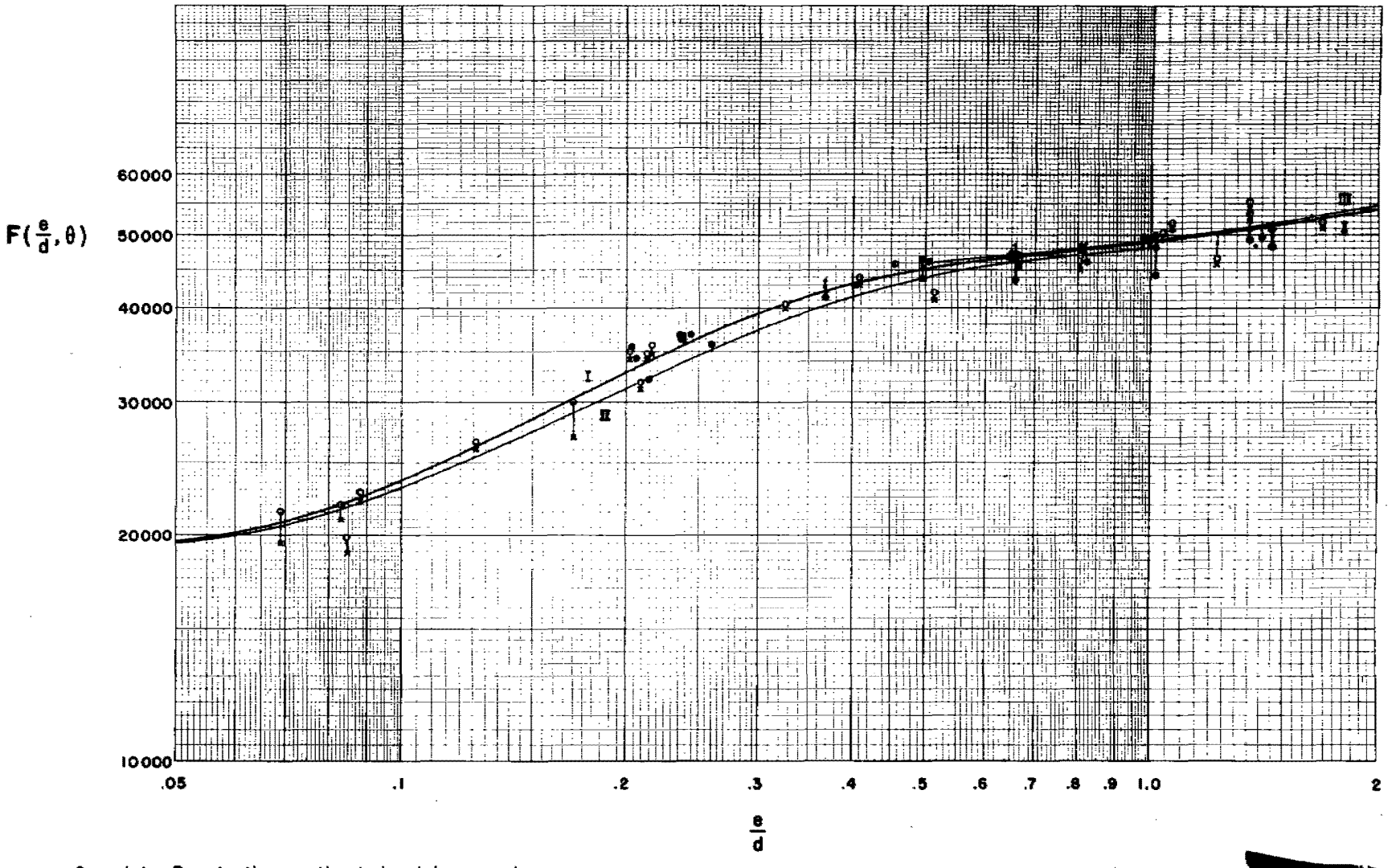

- Complete Penetration, estimated minimum value
- Incomplete Penetration, estimated maximum value
- Limit Determination, uncorrected
- Limit Determination, corrected

CURVE I	Standard	3" AP M79 Projectile
CURVE II	Theoretical	Thin Plate
CURVE III	Theoretical	Thick Plate

NPG PHOTO NO. 2979 (APL)

PLATE PENETRATION COEFFICIENTS

FIGURE (3)

Small Caliber Monobloc Projectiles vs Homogeneous Plate at 0° Obliquity, corrected for Scale, Ogive, and Tensile Strength, to 3" Scale, 1.67 Caliber Ogival Radius, and 115000 (lb)/(in)^2 Tensile Strength

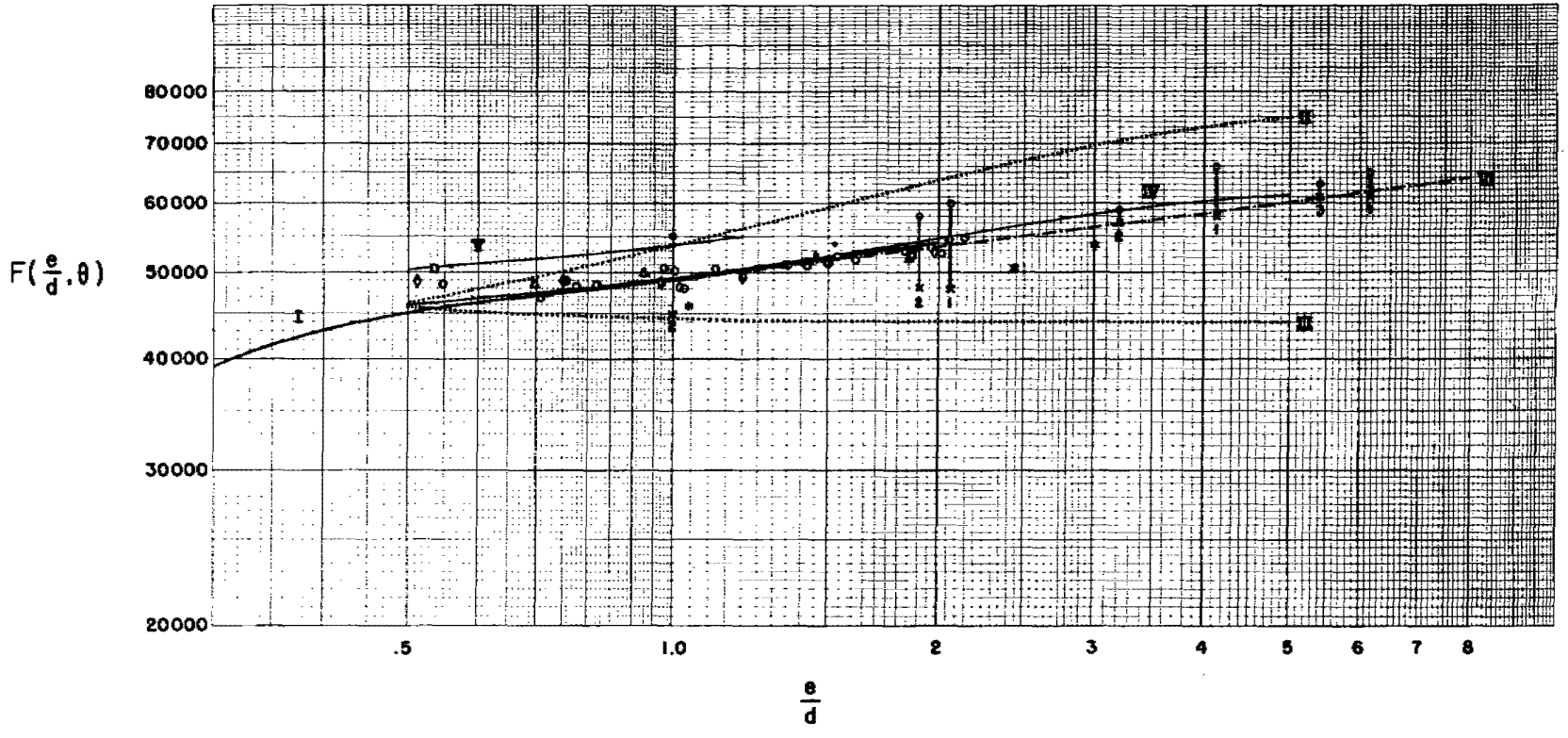

Symbol	Caliber	Type	Ogival Radius	Carrier
o	.303 to 40mm	2 pdr models	1.4 Cal	Plating or Band
•	.60	FA Dw 51	1.67 Cal	Base Cup
△	.27	Steel Dart	2.5 Cal	None
□	.30	AP M2 Dart	3 Cal	None
*	.30	AP M2 Dart	3 Cal	Cal .50 Arrowhead
⊗ 1	.30	M-24-20	1.25 Cal	Cal .50 Sabot
◊	.50	E5, E6	1.5 Cal	Rotating Band
⊗ 2	20mm	M-20mm-2	1.5 Cal	Base Cup or Sabot
⊗	[illegible]	Mk I Type 860	1.4 Cal + 80° Cone	Sheath and Sabot

Curve I	Experimental	3" AP M79 Projectile
Curve II	Theoretical	Irrotational Flow with Fault Formation
Curve III	"	Equilibrium Flow with Fault Formation
Curve IV	"	Thick Plate with Fault Formation
Curve V	"	Thick Plate without Fault Formation
Curve VI	Empirical	from Princeton Station Formula
	$(10^{-8})U(\frac{e}{d},\theta) = 24(\frac{e}{d})^{1.26}$	

NPG PHOTO NO. 3048 (APL)

FIGURE (4)

THE OBLIQUITY FUNCTION Θ

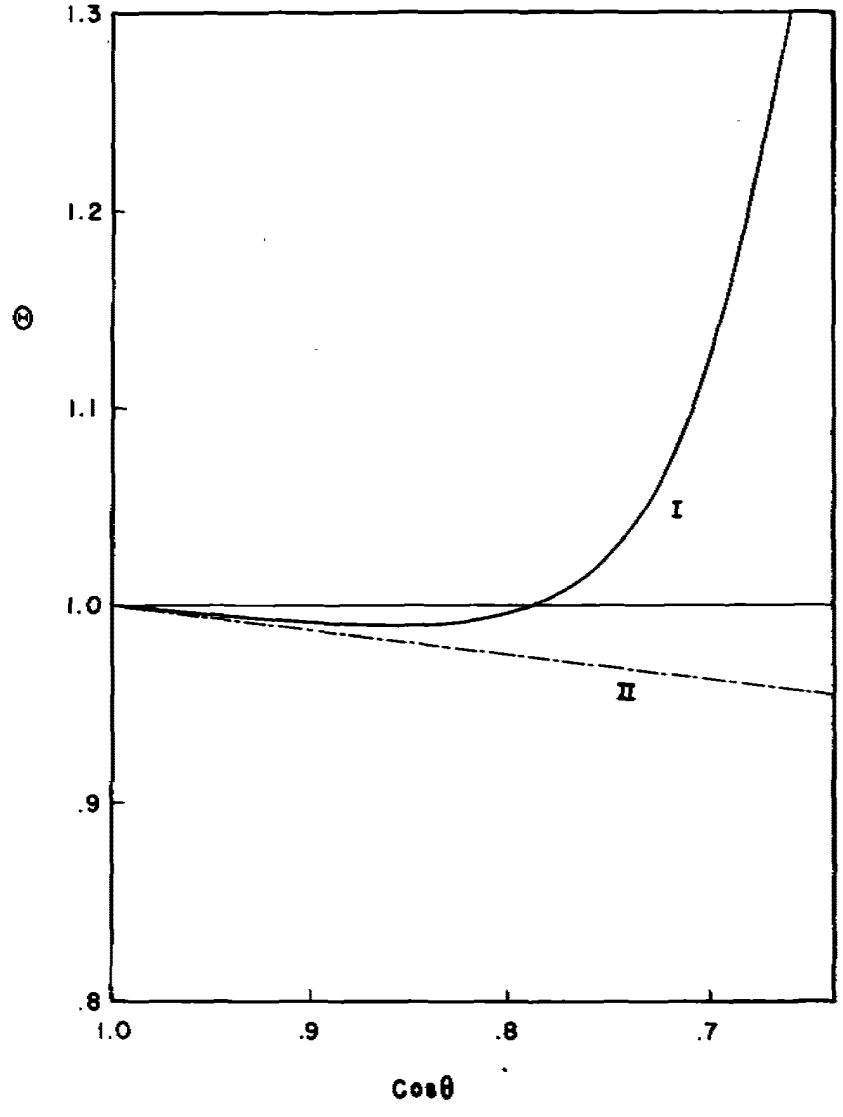

CURVE I Experimental
3" AP M79 Projectile

CURVE II Theoretical
Thick Plate without Ricochet

NPG PHOTO NO. 3096 (APL) FIGURE (5)

THE DEPTH OF PENETRATION

3" AP Type A Projectile in Homogeneous Plate at Low Obliquity

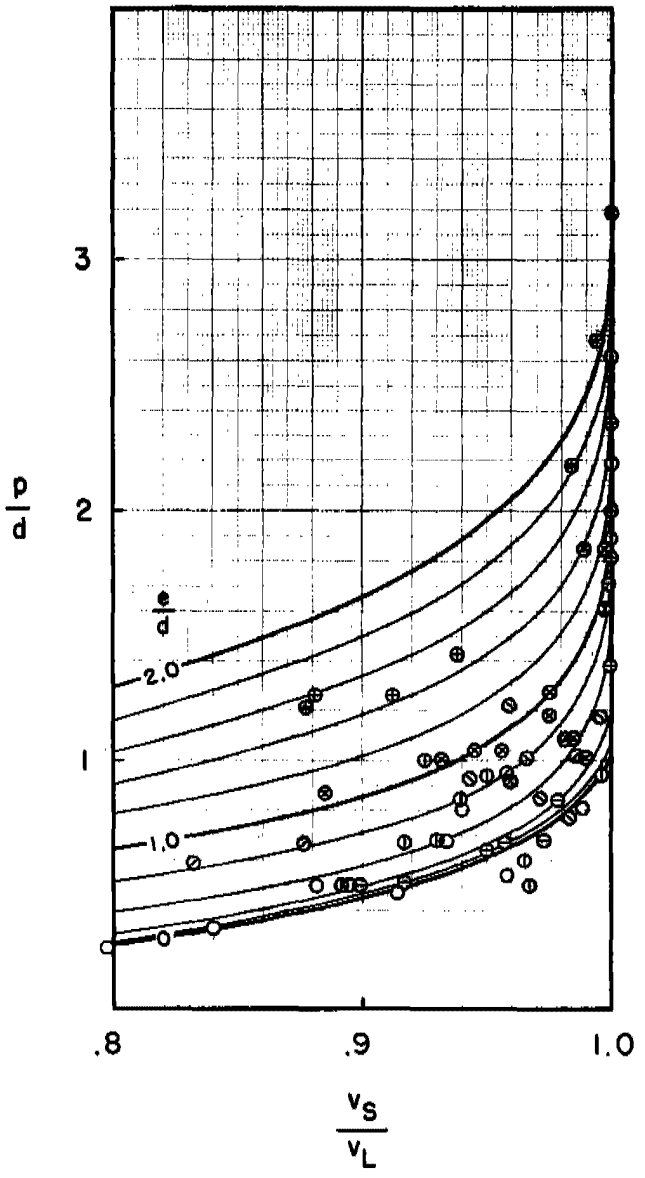

e = plate thickness

d = projectile diameter

p = depth of penetration

v_S = striking velocity

v_L = limit velocity

Symbol	e/d
○	.004
◐	.25
⊖	.40
⊘	.65
⊘	.82
⊗	1.00
✇	1.17
⊕	1.38
⊛	1.73

NPG PHOTO NO. 3097 (APL)

FIGURE (6)

THE DEPTH OF PENETRATION

3" AP M79 Projectile in Homogeneous Plate at Low Obliquity

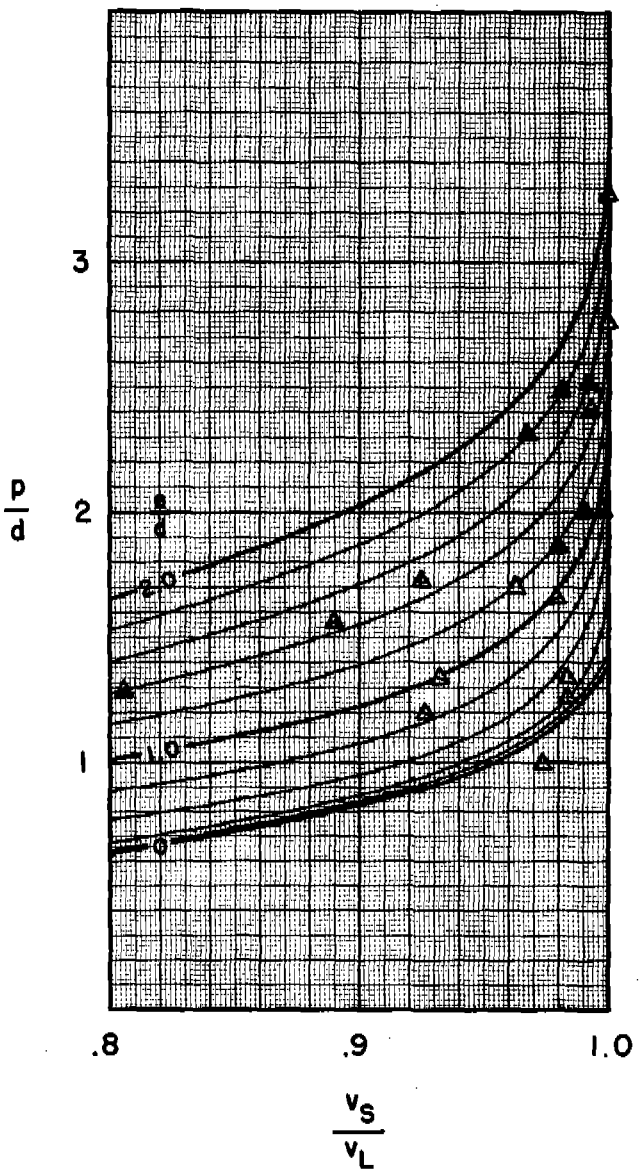

e = plate thickness

d = projectile diameter

p = depth of penetration

v_S = striking velocity

v_L = limit velocity

Symbol	e/d
△	.49
△	.65
△	.82
△	1.00
△	1.36
△	1.62

NPG PHOTO NO. 3164 (APL)

EFFECT OF OGIVE ON THE DEPTH OF PENETRATION

FIGURE (7)

3" Projectiles in Homogeneous Plate No. D037

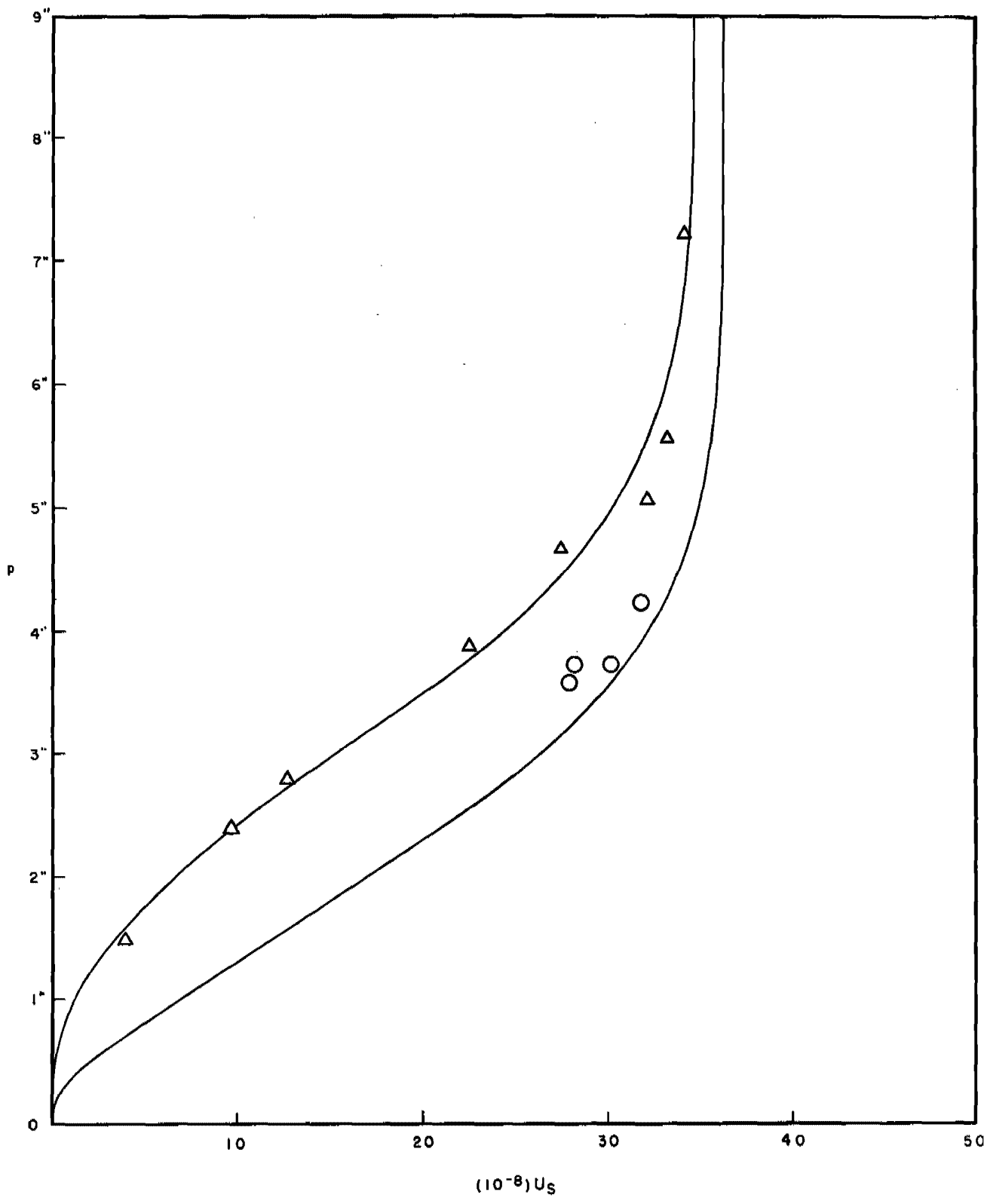

○ 3" AP Type A Projectile

△ 3" AP M79 Projectile

$\frac{e}{d} = 1.38$

NPG PHOTO NO. 3165 (APL)

FIGURE (8)

THE FORCE ON THE 3" AP M79 PROJECTILE AT e/d = 0.25

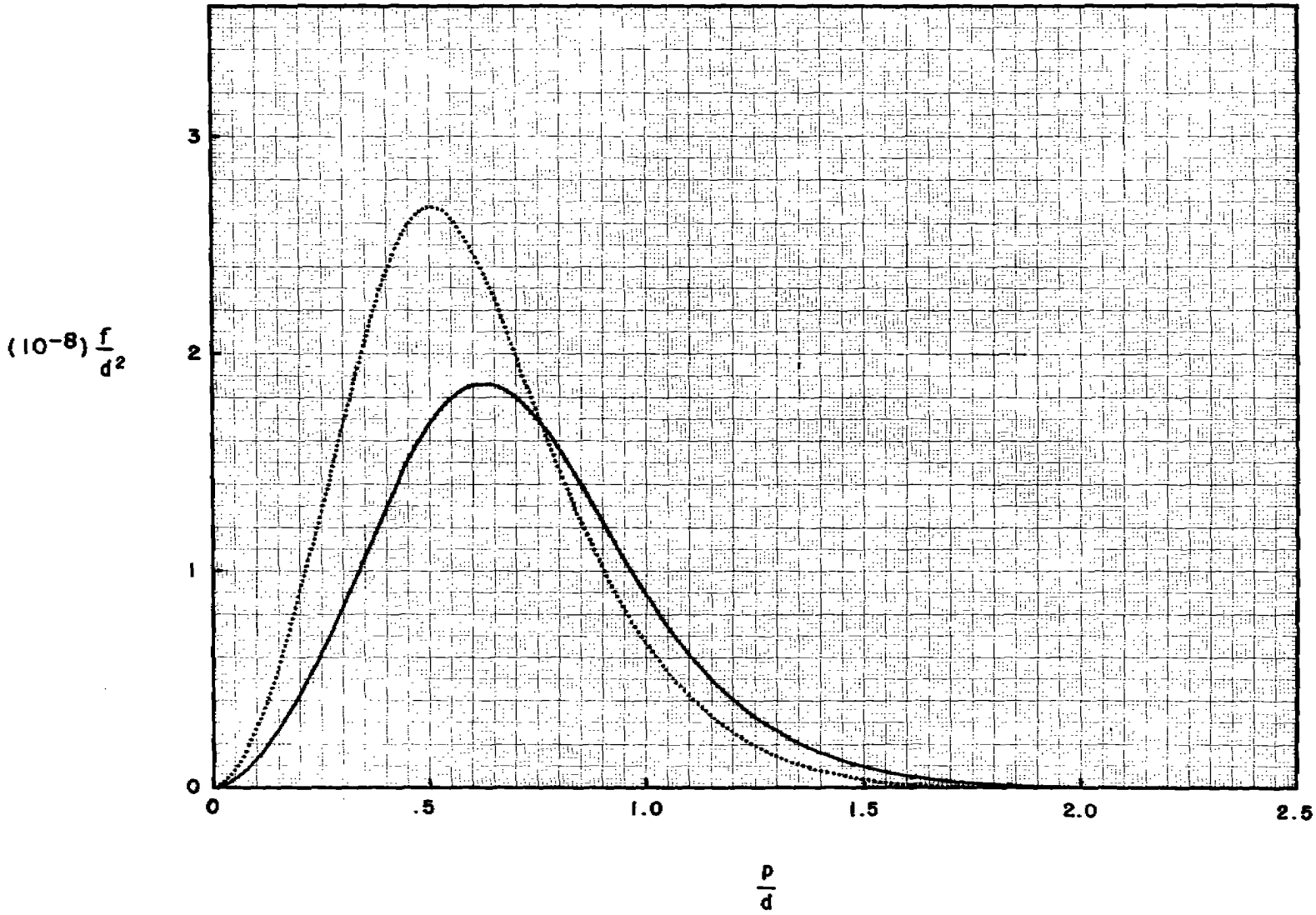

NPG PHOTO NO. 3166 (APL)

FIGURE (9)

THE FORCE ON THE 3" AP M79 PROJECTILE AT e/d = 1.0

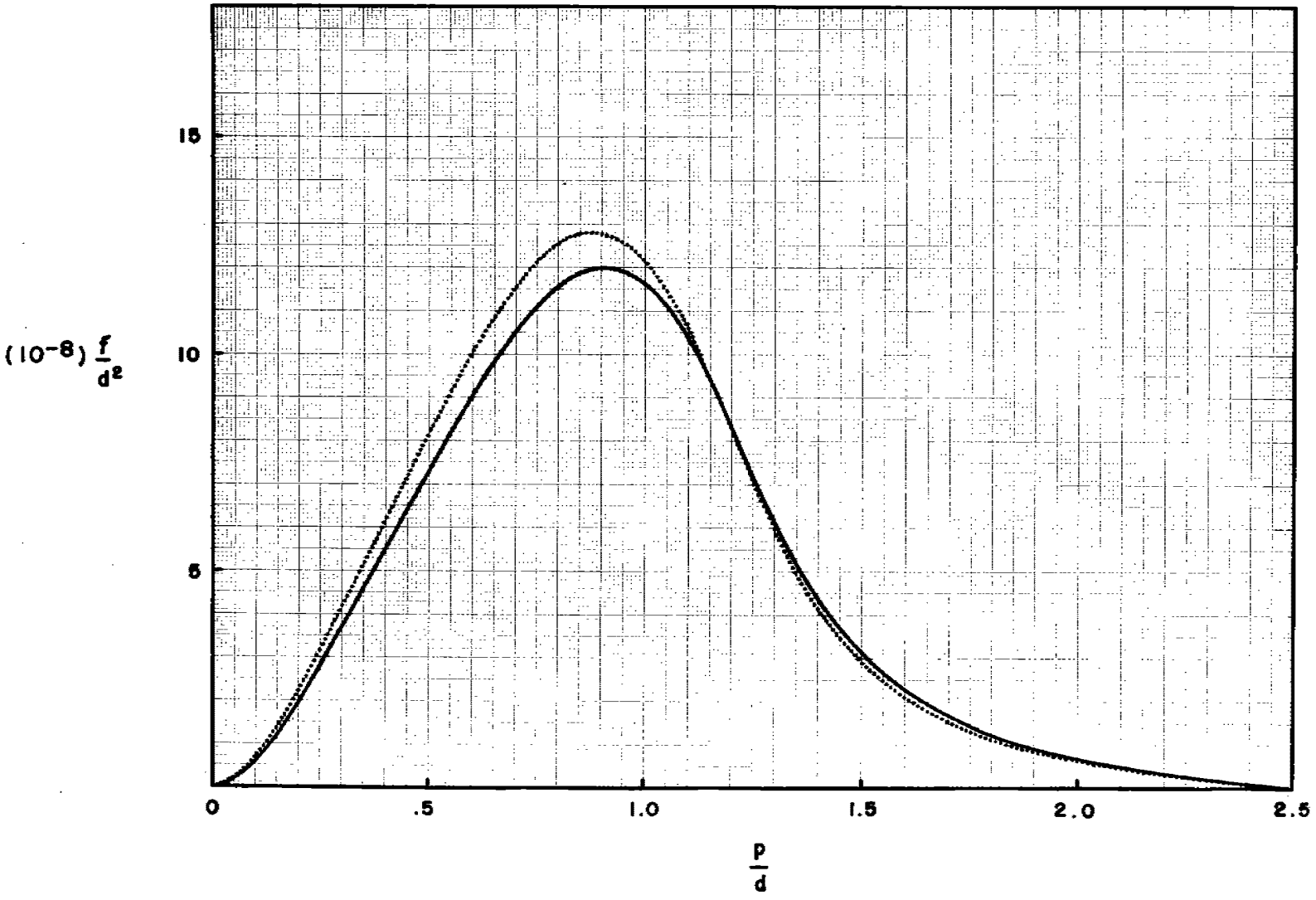

ABSORPTION DATA FOR OBLIQUE IMPACT

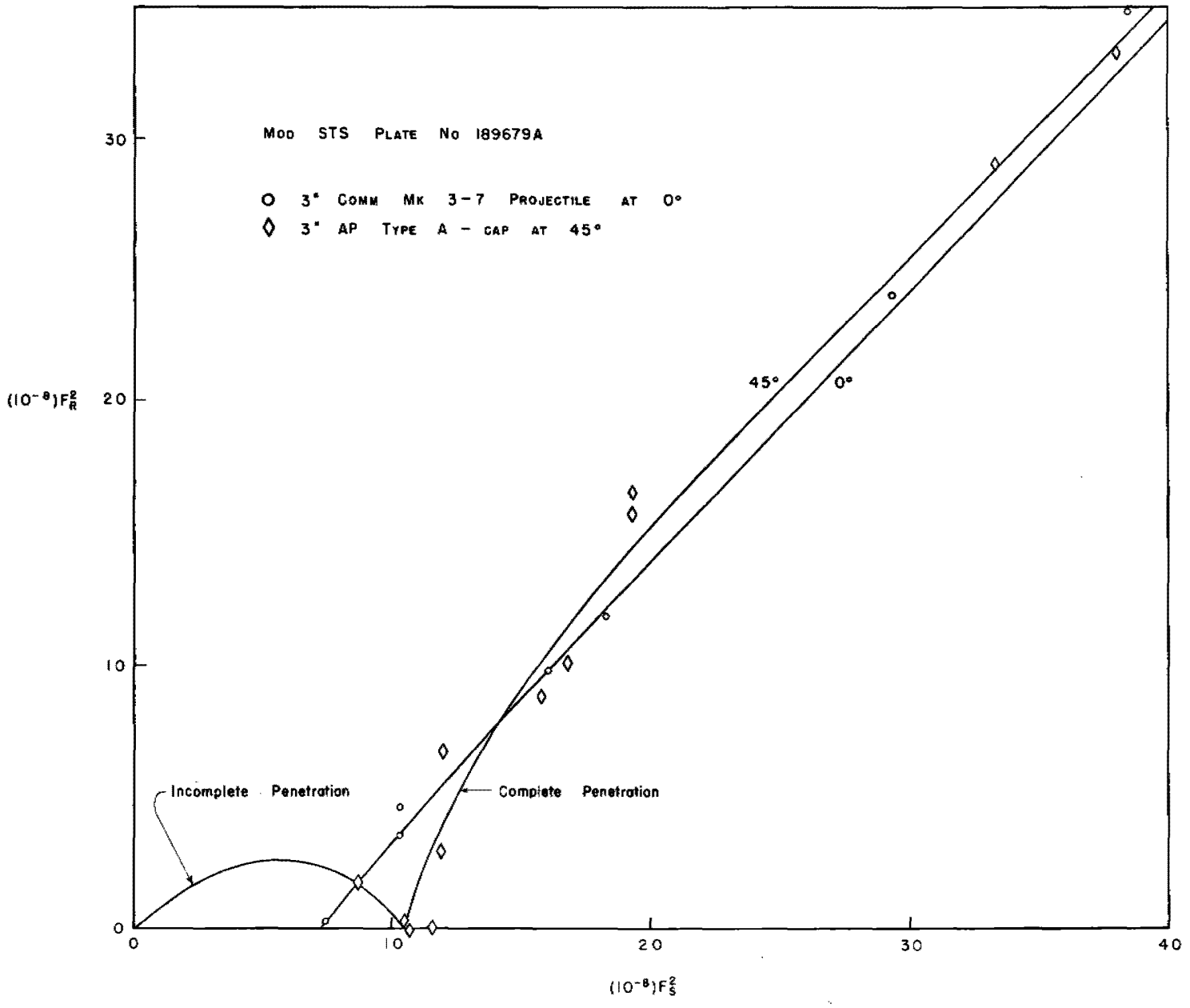

NPG PHOTO NO. 3168 (APL)

ABSORPTION FUNCTIONS

FIGURE (11)

3" AP M79 Projectile in Homogeneous Plate at 0° Obliquity

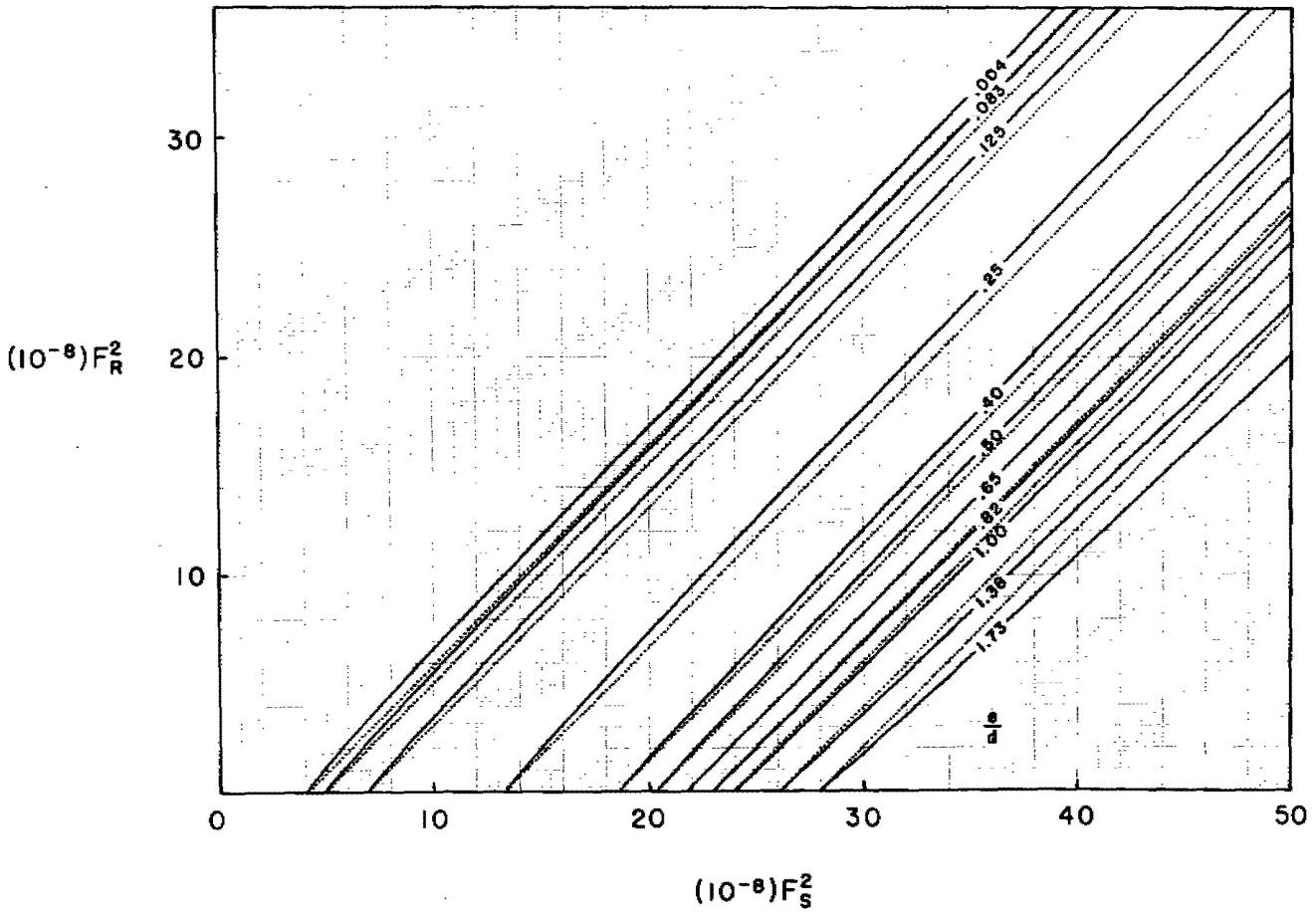

m = projectile mass (lb)

d = projectile diameter (ft)

e = plate thickness (ft)

θ = obliquity

v_S = striking velocity (ft)/(sec)

v_R = remaining velocity (ft)/(sec)

$$F_S^2 = \frac{mv_S^2\cos^2\theta}{ed^2}$$

$$F_R^2 = \frac{mv_R^2\cos^2\theta}{ed^2}$$

ABSORPTION DATA FOR 0° OBLIQUITY

FIGURE (12)

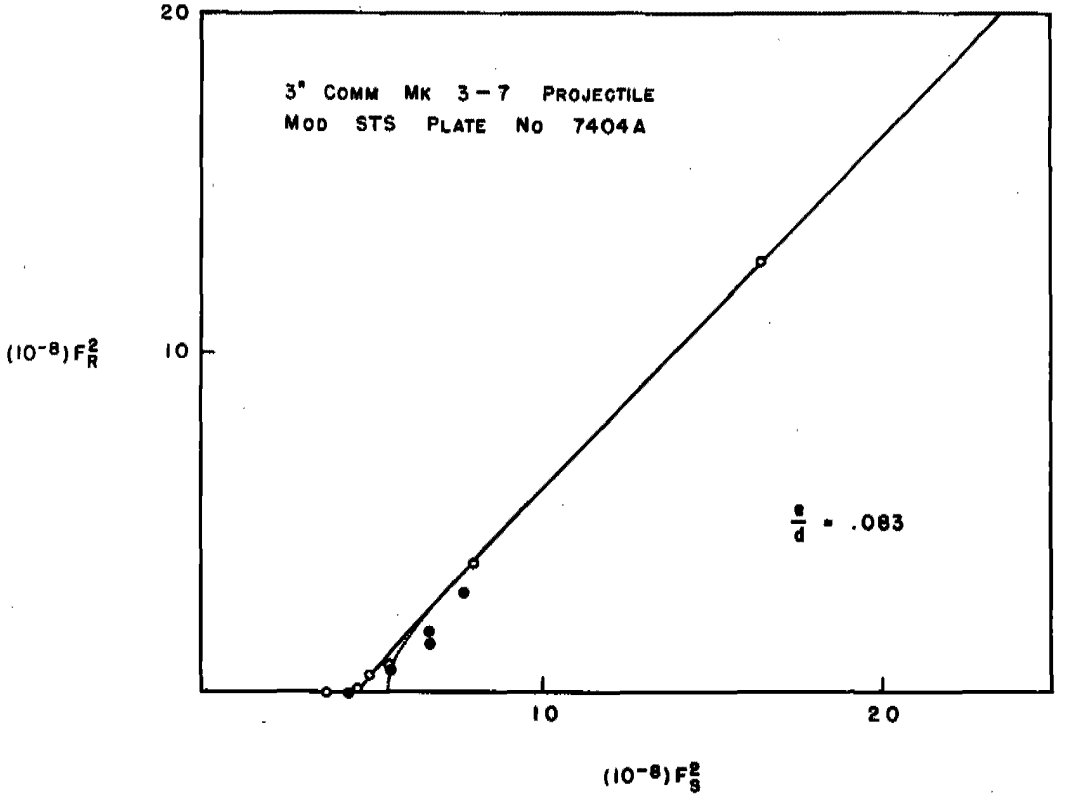

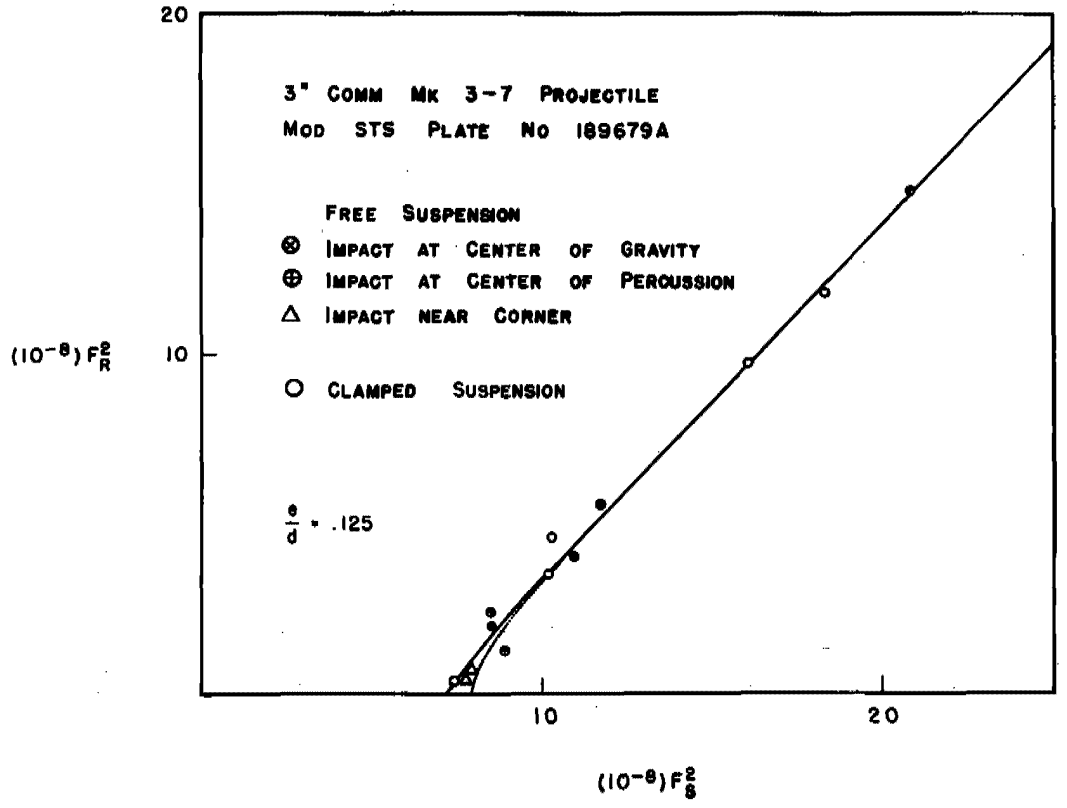

ABSORPTION DATA FOR OBLIQUE IMPACT

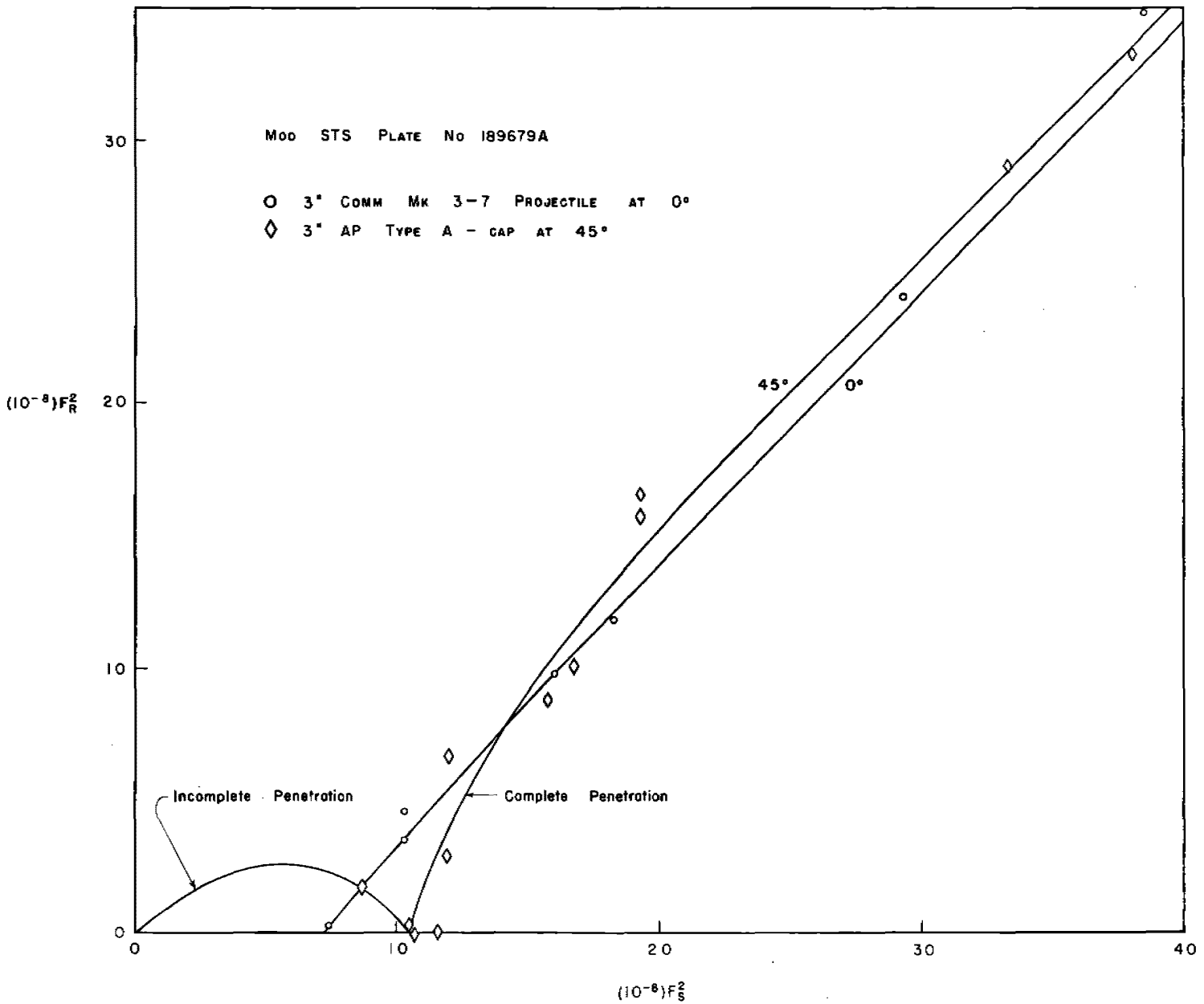

NPG PHOTO NO. 3156 (APL)

FIGURE (14)

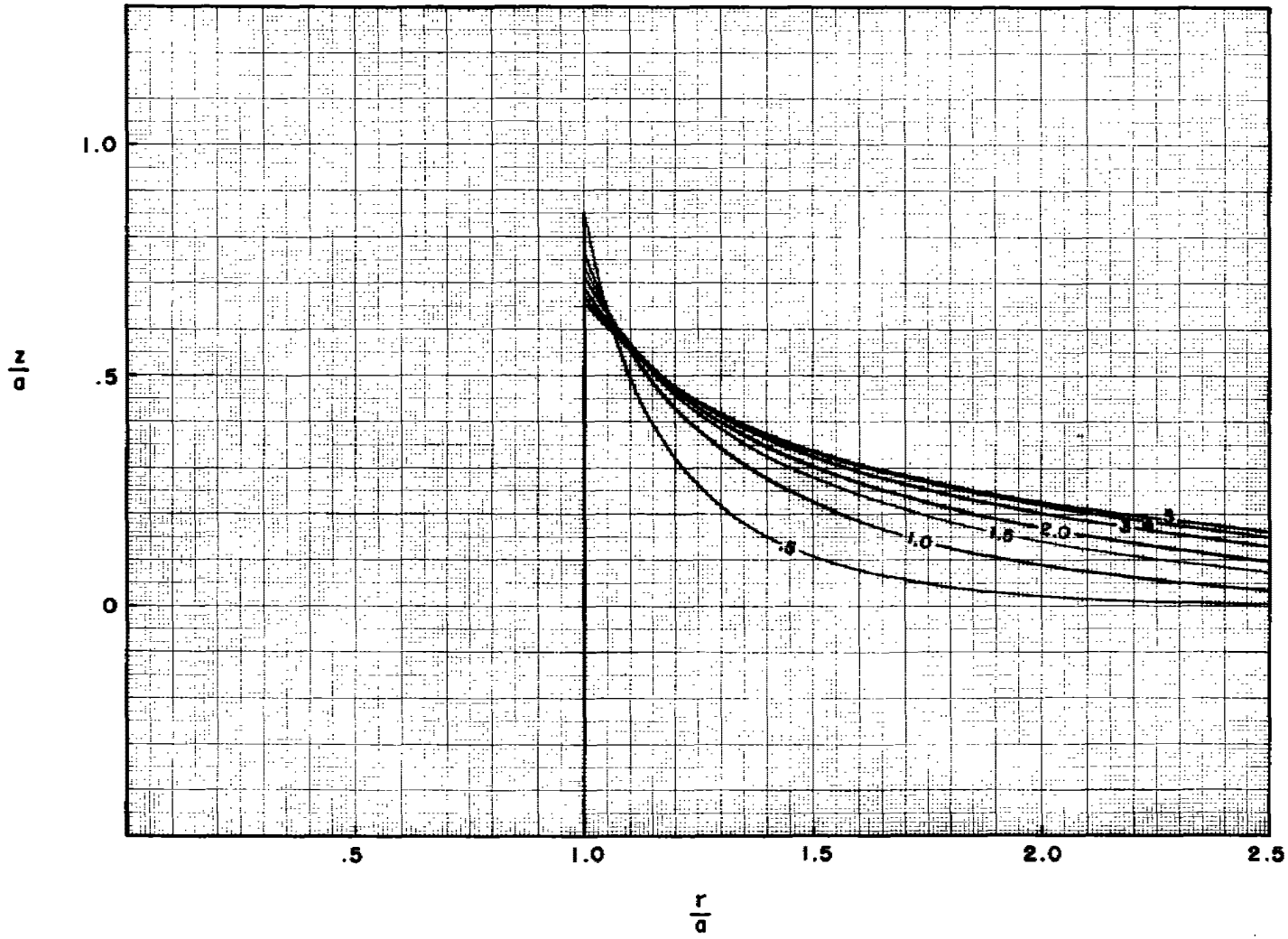

COMPARISON OF THE SURFACE CONTOURS OF PLATES OF VARIOUS CALIBERS THICKNESS – IRROTATIONAL FLOW FROM CONSECUTIVE COAXIAL CYLINDERS OF ALTERNATE SIGN

NPG PHOTO NO. 3157 (APL)

FIGURE (15)

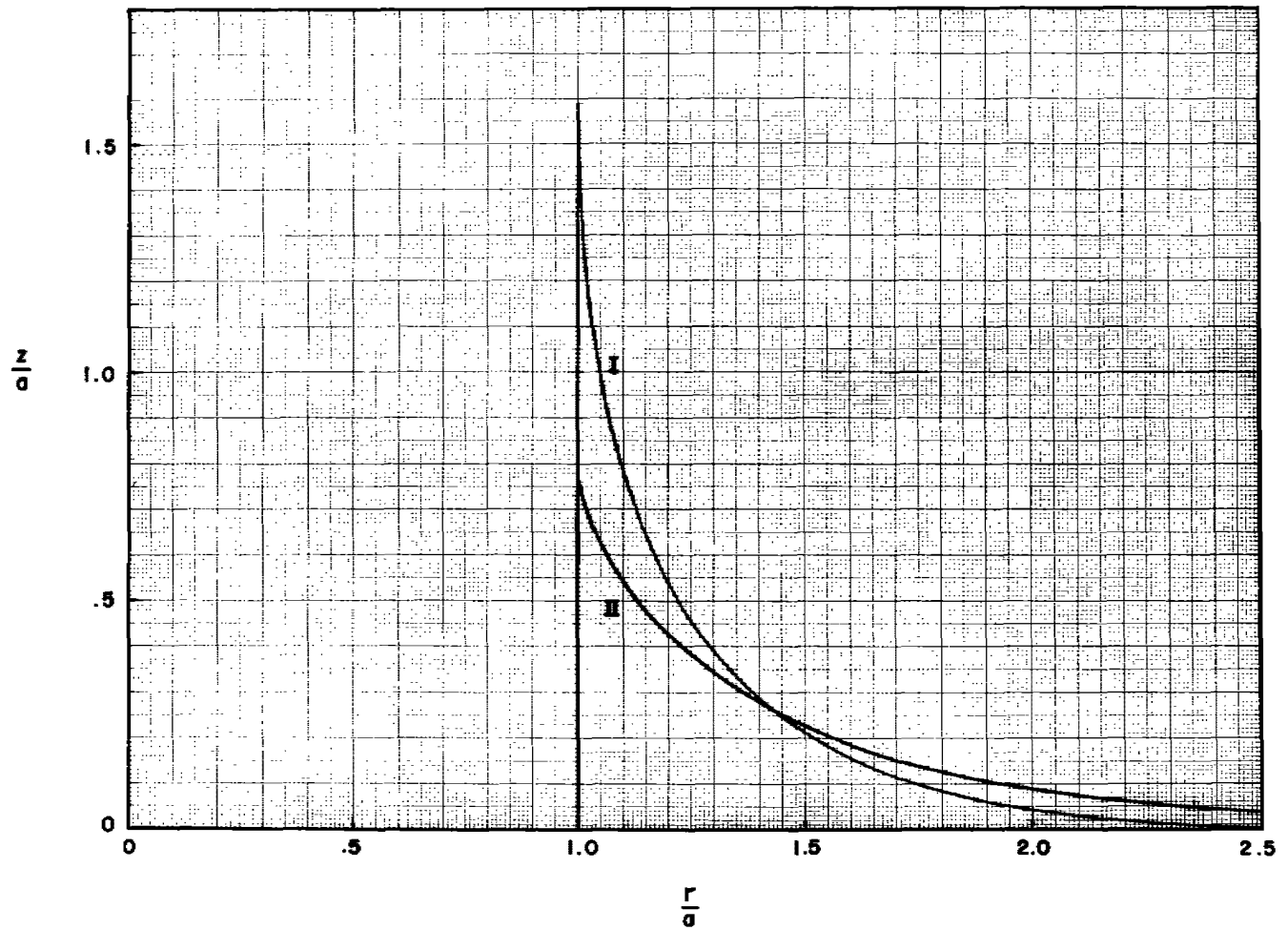

COMPARISON OF THE SURFACE CONTOURS FOR EQUILIBRIUM FLOW AND IRROTATIONAL FLOW IN A PLATE OF CALIBER THICKNESS

Curve I Equilibrium Flow

Curve II Irrotational Flow

NPG PHOTO NO. 3171 (APL)

FIGURE (16)

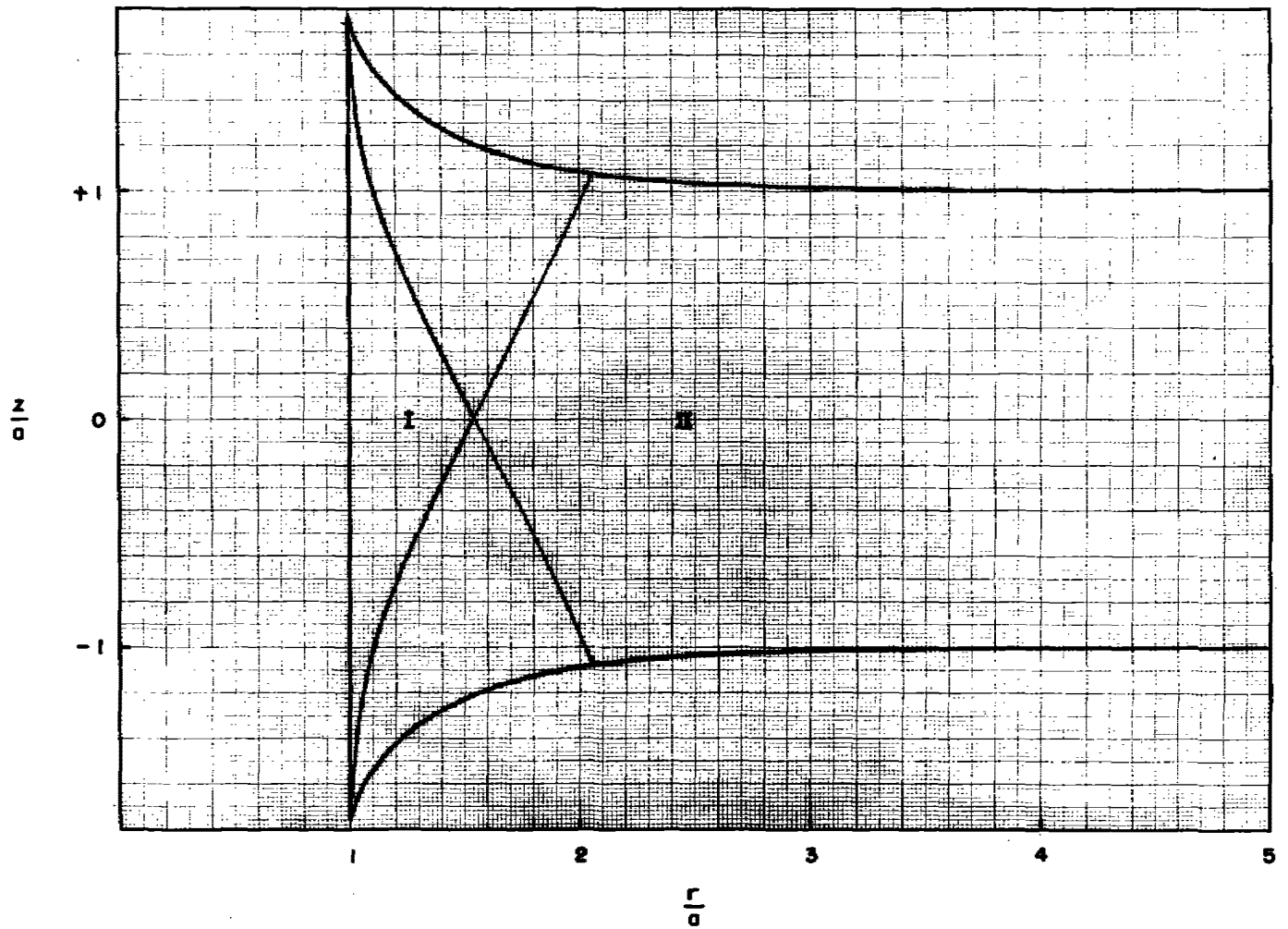

THE ZONES OF IRROTATIONAL FLOW AND EQUILIBRIUM FLOW

IN A PLATE OF CALIBER THICKNESS

Zone I Irrotational Flow

Zone II Equilibrium Flow

NPG PHOTO NO. 3163 (APL)

FIGURE (17)

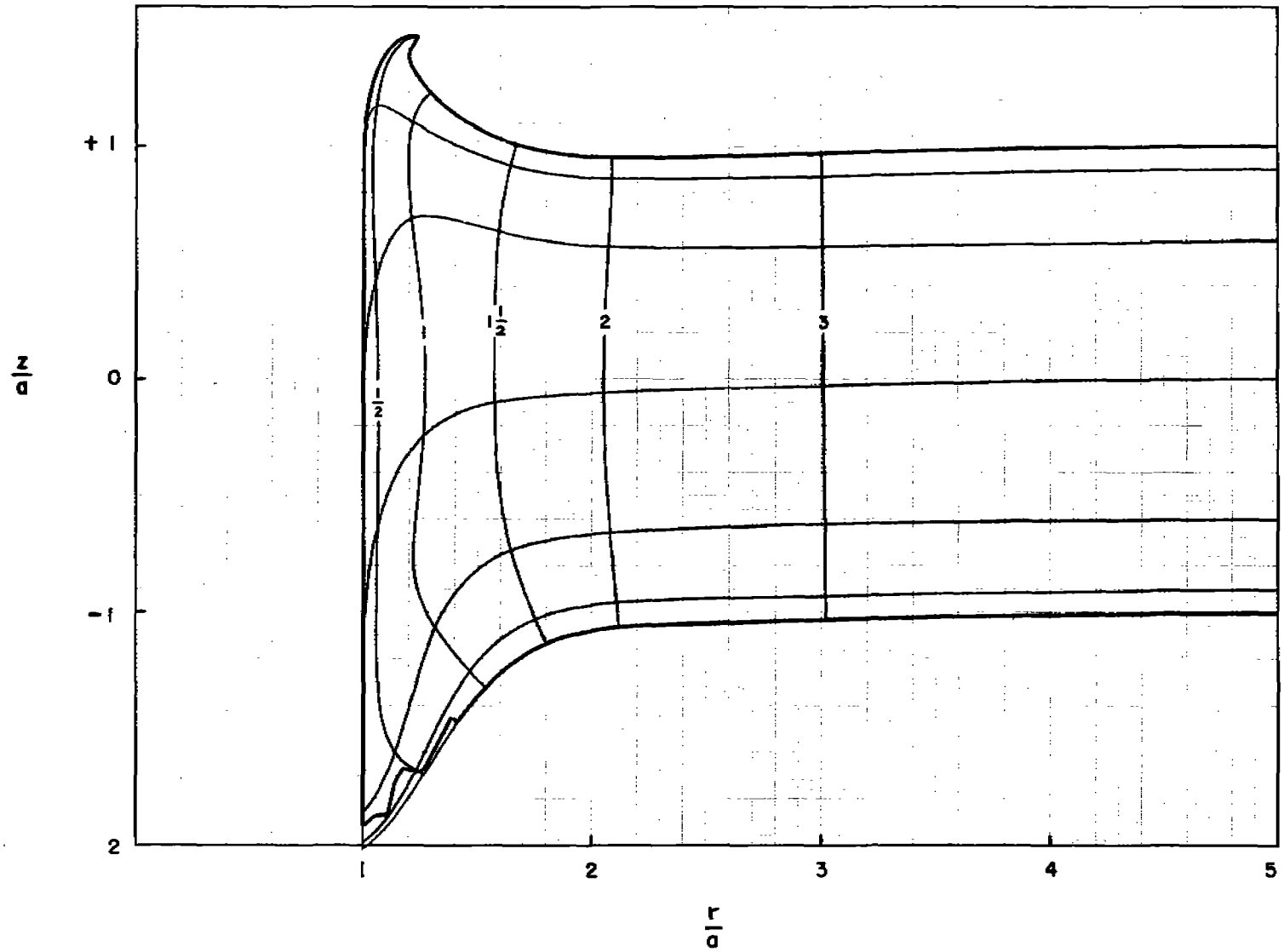

THE DEFORMATION CONTOURS FOR A 3" AP M79 PROJECTILE IN A PLATE OF CALIBER THICKNESS

Classification:

STI **ATI No.** 203 990

O.A. NPG

O.A. No. Rept 9-46

Title Analytical summary pt IV the theory of Armor penetration

Author(s)

Date 1 May 46

P.A.

P.A. No.

CADO Form No. 49